Quantum Mechanical Calculation of NMR Parameters in the Stereostructural Determination of Natural Products

Simone Di Micco,[a] Maria Giovanna Chini,[a] Raffaele Riccio,[a] and Giuseppe Bifulco*[a]

The present microreview highlights the recent goals reached by the application of a combined approach of NMR spectroscopy and quantum chemical methods in the structural studies of natural products. In particular, different case studies are reported, showing the comparison of calculated NMR parameters at the quantum mechanical (QM) theory level with experimental data for the configurational assignment of organic compounds. Moreover, it is shown that the QM–NMR approach can be used as a fast and convenient method to lead the total synthesis of complex natural products to the correct stereoisomer. Through recent analysis of the covalent complex formed between d(GACTAATTGAC)-(GTCAATTAGTC) and (+)-yatakemycin, the potential application of this hybrid method as a useful tool for the characterization of bioactive molecule–biopolymer interactions is presented.

1. Introduction

Many molecular properties of organic compounds, such as chemical reactivity, catalytic, biological, and pharmacological activities, are critically affected not only by their functional groups but also by their spatial position. Thus, the disclosure of the relative configuration has a great impact in the full understanding of their chemical behaviors. Different approaches to determine the exact structure and/or configuration of organic products have been devised.[1–3] Total synthesis has played a primary role in structural assignment and revision but its drawback is represented by the additional costs in terms of time and money. For these reasons, a series of new and more rapid methods, such as nuclear magnetic resonance (NMR), circular dichroism (CD), X-ray crystallography, and mass spectrometry (MS), which allow preservation of the sample under investigation, have shown to be valid alternatives to classical chemical approaches.

In this field, NMR spectroscopy is one of the most employed tools, as some NMR parameters [coupling constant, chemical shift (cs)] can provide fundamental information on the configurational and conformational arrangement of organic molecules. For example, the $^3J_{H,H}$ coupling constants between protons separated by three bonds depend on the dihedral angles, following the well-known Karplus equation.[4] Moreover, the nuclear Overhauser effect (NOE)[5] provides information of the 3D spatial arrangement of the nuclei, clarifying the geometrical information on the relative positions of the atoms in the analyzed molecule. Thus, the evaluation of simple NMR parameters, such as proton–proton J coupling values, chemical shifts, and/or nuclear Overhauser effect intensities, allows the configuration of cyclic compounds with three- to six-membered rings, and of compounds with predictable conformational behavior, to be determined. Polysubstituted open chains and macrocycles constitute more difficult cases of relative configurational assignment, because stereochemical analysis is complicated by geometrical uncertainty of such types of flexible systems.

For the above situations, different NMR-based methods, such as J-based analysis,[3,6] the universal NMR database (UDB),[3,7] and the quantum mechanical calculation of NMR parameters,[3,8] have been proposed for the relative (and/or absolute) configurational assignment of organic molecules. J-Based analysis was originally devised by Murata and co-workers, and it has been shown to be very helpful for the relative configurational assignment of two adjacent (1,2) or alternate (1,3) stereocenters belonging to an acyclic carbon chain. Briefly, this J-based approach consists in considering the three main staggered rotamers (*anti*, g^+, and g^-) of the two possible relative configurations (*threo* and *erythro*) of a stereopair and assigning for each rotamer a predicted qualitative (small, medium, and large) set of $^3J_{H,H}$ and $^{2,3}J_{C,H}$ values based on the dependence of scalar couplings on the dihedral angles. The comparison of the experimentally measured values of homo- and heteronuclear coupling constants with the rotamer-predicted patterns allows the relative configuration of two stereocenters to be assigned.

[a] Department of Pharmaceutical Science, University of Salerno, via Ponte don Melillo, 84084 Fisciano (SA), Italy
Fax: +39-089969602
E-mail: bifulco@unisa.it

The UDB method is based on the comparison of the proton and carbon chemical shifts of a structure having an unknown relative configuration with the resonance values of a molecular database formed by fragments of known compounds. In particular, the structure under study could be divided in small fragments and its chemical shifts compared with an appropriate reference compound in the database.

In the last years, great advances have been made in developing quantum mechanical (QM) methods of chemical interest able to predict molecular properties. In particular, quantum mechanical calculation of NMR parameters has been used as an emerging strategy for the assignment of the relative configuration of organic molecules on the basis of the high accuracy in the reproduction of the experimental NMR properties also achieved at a low level of theory.[9]

For further details about theoretical concepts, applications, and limitations of these NMR-based approaches we refer to our previous review on the determination of the relative configuration of organic compounds.[3] It is noteworthy that besides the development and application of QM approaches for structural studies, fast empirical methods have been devised to predict NMR chemical shifts.[10] These empirical methods are based on fast calculation algorithms[11] that can generate a set of possible structural hypotheses with the average deviation between calculated and experimental chemical shifts equal to $d = 1.8$ ppm for ^{13}C NMR chemical shifts. Such empirical NMR chemical shift predictions could be useful with large-sized molecules or in the presence of very flexible compounds for which different conformers have to be considered in the more time-consuming QM calculations. Moreover, these empirical methods can be ap-

Simone Di Micco was born in Maddaloni, Italy, in 1980. He graduated in Medicinal Chemistry from the University of Naples "Federico II" in 2004. He moved to the University of Salerno, working for one year in the group of Prof. L. Gomez-Paloma on the development of a STD-NMR-based protocol for the screening of DNA ligands. He received his PhD degree from the University of Salerno in 2009 under the supervision of Prof. G. Bifulco. During his PhD studies, he was a visiting scientist at the Burnham Institute for Medical Research (La Jolla, CA) in the group of Prof. Maurizio Pellecchia, working on the design of new Bcl-x$_L$ inhibitors. For his work at this institute he was awarded the EMBO fellowship. He is now a postdoctoral associate at the University of Salerno, conducting research in the group of Prof. G. Bifulco. His research activities are focused on studying drug–macromolecule interactions by NMR spectroscopy and computational chemistry methods in addition to configurational and conformational studies of bioactive compounds by quantum mechanical calculation of NMR parameters.

Maria Giovanna Chini was born in Naples, Italy, in 1981. She graduated in Medicinal Chemistry, summa cum laude, from the University of Naples "Federico II" in 2005. From 2006–2009 she had a fellowship funded by POR Campania 2000–2006, PRIN 2006, and the Department of Pharmaceutical Sciences of University of Salerno under the supervision of Prof. G. Bifulco, working on the design of new antitumor and anti-inflammatory drugs and quantum mechanical calculations for configurational analysis of natural products. In 2008, she obtained a specialization in Farmacia Ospedaliera at the University of Naples "Federico II". Currently, she is a PhD student at the University of Salerno in the group of Prof. G. Bifulco with a project entitled "Design of new molecules with potential anticancer activity".

Raffaele Riccio was born in Naples, Italy, in 1948. After obtaining a doctorate in Chemistry in July 1972 from the University of Naples, he was appointed as Ricercatore of the Consiglio Nazionale delle Ricerche at the Istituto per la Chimica di Molecole di Interesse Biologico in 1973. He spent a year (1976–1977) in a postdoctoral position with P. J. Scheuer at the University of Hawaii. From 1981 to 1990 he moved as a visiting scientist to various international departments [1981 – Department of Chemistry, Cornell University, Ithaca, N.Y., Prof. J. Clardy; 1981 – Department of Chemistry, Columbia University, New York, N.Y., Prof. K. Nakanishi; 1990 – Scripps Institution of Oceanography, University of California San Diego, La Jolla, California, Prof. W. Fenical; 1993 – Department of Chemistry, University of Hawaii at Manoa, Honolulu, Hawaii, Prof. P. J. Scheuer]. From 1987–1994 he was Associated Professor of Organic Chemistry, Faculty of Pharmacy, University of Napoli and in 1995 he moved to the Faculty of Pharmacy of the University of Salerno as a Full Professor. He is currently Dean of the Faculty of Pharmacy of the University of Salerno. His research activities have been mainly devoted to the discovery and to the chemical and pharmacological investigation of new bioactive natural products as "lead compounds" in the area of antiviral, antitumoral, anti-inflammatory, and immunomodulant activities.

Giuseppe Bifulco was born in Naples, Italy, in 1968. He obtained his PhD from the University of Naples, working in the Organic Chemistry group of Prof. Minale in 1996. He was a visiting scientist at the Scripps Research Institute (San Diego, CA) under the supervision of Prof. W. J. Chazin, working on calcium-binding proteins (1994–1995, 1996, and 1998) and with Prof. K. C. Nicolaou, working on the interactions between synthetic dimers of calicheamicin and DNA (1995, 1996, 1998). From 1997 to 1999 he was a postdoctoral student at the University of Salerno in the group of Prof. Riccio; from 1999 to 2005 he was a Researcher at the University of Salerno, where he focused his attention on the study of marine and terrestrial natural products, in particular putting his efforts in the structural characterization of the products by using homonuclear and heteronuclear one- and two-dimensional NMR techniques. Currently, he is an Associate Professor at the Department of Pharmaceutical Science of the University of Salerno. He is involved in several research fields: structural characterization of biologically active natural organic compounds from marine and terrestrial sources; advanced NMR techniques in organic chemistry; quantum mechanical calculation for the determination of the conformation and the configuration of natural compounds; structural studies on drug–DNA interactions; molecular docking and antitumor drug design. He was awarded in 2004 with the Italian Chemical Society "G. Ciamician" medal, a national prize for researchers.

plied as a filter to narrow the number of stereoisomers to be accurately verified by other methods such as X-ray, total synthesis, and QM approaches.

The ^{13}C-based protocol (Figure 1), proposed by our research group, consists of four fundamental steps: (a) conformational search and preliminary geometry optimization of all the significantly populated conformers of each stereoisomer; (b) final geometry optimization of all the species at the QM level; (c) GIAO (gauge including atomic orbital)[12] ^{13}C NMR calculations of all the so-obtained structures at the QM level; (d) comparison of the Boltzmann-averaged NMR parameter calculated for each stereoisomer with those experimentally measured for the compound under examination. This protocol has been devised for flexible systems considering the importance of the contribution of all significant conformers to predict a chemical–physical property and the theory level used to calculate the energy of the single geometrical isomers.[8] Considering the simple case of a molecule with a couple of two adjacent stereocenters, the first step is to build two diastereoisomers by dedicated software. The conformational sampling is performed at the empirical theory level,[13] generally through molecular dynamics (MD) or by Monte Carlo multiple minimum methods (MCMM).[14]

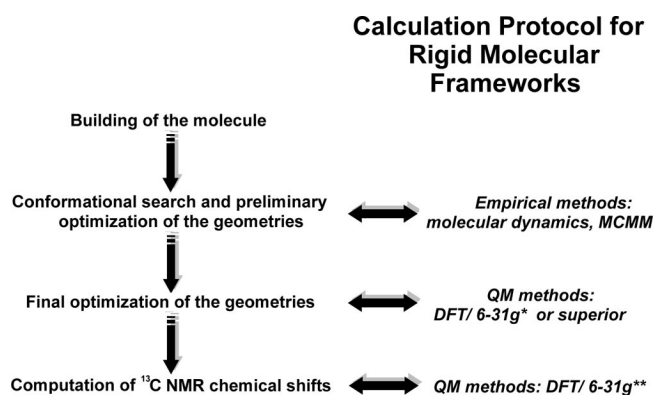## Calculation Protocol for Rigid Molecular Frameworks

Figure 1. Schematization of the protocol used for the determination of the relative configuration in organic compounds based on calculation of ^{13}C NMR chemical shifts at the QM level of theory.

A preliminary geometry optimization is run at the empirical (molecular mechanics, MM) or semiempirical level (AM1,[15] PM3,[16] or other) on all found conformers for each diastereoisomer, followed by a QM optimization step. On the so-obtained geometries, the ^{13}C NMR chemical shift for each stereoisomer is calculated and the theoretical data are extrapolated by taking into account the Boltzmann-weighted average derived from the energies of the single conformers. The calculated values are compared with the experimental NMR spectroscopic data and the relative (or absolute) configuration is determined based on the best fit between the theoretical and experimental data set given by one of the two structural hypotheses.

Following the same key steps described for the ^{13}C-based protocol, the calculation of homo- and heteronuclear coupling constants can be carried out for the conformational

and configurational studies of organic molecules. In detail, each global minimum conformer undergoes full geometry optimization by using the DFT theoretical level[17] and then, on the obtained geometries, the calculation of the J couplings is performed by taking into account the contributions of the following interactions: Fermi contact (FC), paramagnetic spin–orbit (PSO), diamagnetic spin–orbit (DSO), and spin–dipole (SD). On the basis of the Boltzmann distribution of the conformers, the calculated J coupling values are extrapolated and then compared to the experimental data set, suggesting the relative configuration of the examined compound. For large molecular systems, presenting many stereocenters, it is suggested that, given the prohibitive computational requirement for simultaneous consideration of all combinations of the possible conformations and configurations, the molecule can be dissected into appropriately 2-C fragments prior to the J coupling calculations,[18] as for the Murata method.[6] Each reduced subsystem is treated like an entire molecule: a geometry optimization step, followed by $^3J_{H,H}$ and $^{2,3}J_{C,H}$ calculations, is performed for each staggered rotamer. It is only one of the six calculated data sets that should display a satisfactory agreement with the experimental values. Differently from the original J-based approach proposed by Murata,[6] for which it is impossible to distinguish the *anti erythro* from the *anti threo* arrangement on the basis of the sole evaluation of the J coupling values, the quantitative analysis of the calculated versus the experimental data allows the relative configurational assignment for the correct *anti* rotamer. In this review, we particularly focus on the use of NMR parameter calculations at the QM theory level in the determination of relative configuration, but many other applications of QM methods in structural studies are reported in the literature. The high reliability of the NMR properties predicted by QM methodologies can be a powerful tool in the structural elucidation process of natural compounds.[19] Indeed, recently, Rychnovsky revised and reassigned the structure of the natural product hexacyclinol on the basis of quantum chemical calculation of ^{13}C NMR chemical shifts.[20] Similarly, Zhao proposed a new structure of hassananes[21] with a diterpenoid skeleton, isolated from the plant *Salvia apiana*. Moreover, other examples are represented by the investigation of the conformational behavior, along with the spectroscopic properties, of 4′-epiadriamycin[22] and (+)-yatakemycin[23] through the DFT theory[17] level.

In the next paragraphs examples of relative configurational assignment by QM calculation of ^{1}H and ^{13}C NMR chemical shifts will be reported, whereas in sections 3.1–3.3, 3.5, and 3.6 the applications of calculated J coupling constants will be shown. Different combinations of calculated NMR properties for structural studies of organic molecules will be presented in section 3.4. In section 4, the QM approach will be indicated as a powerful tool for the selection of stereostructures prior to their total synthesis. Recently, we applied QM calculation of ^{1}H NMR chemical shifts for the analysis of the covalent complex formed between (+)-yatakemycin and the d(GACTAATTGAC)-

(GTCAATTAGTC) duplex (section 5), showing that the calculated NMR parameters can be a useful tool for the structural characterization of ligand–macromolecule interactions.[24]

## 2. Quantum Mechanical Calculation of NMR Chemical Shifts

2.1 QM Calculation of ^{13}C NMR Chemical Shifts for the Stereochemical Assignment of Bonannione B

Analysis of the relative configuration of the flavonoid bonannione B (**1**, Scheme 1), isolated from the plant *Bonannia graeca*, is reported[25] as a straightforward application of ^{13}C NMR chemical shift calculation. As the stereopair (C-2″ and C-3″) under investigation is only partially constrained, the configuration could not be deduced by simple analysis of the 2D ROESY spectra. Moreover, due to the small amount of the isolated compound, it was not possible to apply Mosher's method,[26] so the only feasible strategy was to use ^{13}C values calculated at the QM theoretical level. QM–NMR structural analysis of **1** was carried out by taking into consideration all three staggered rotamers (two *gauche* and one *anti*, Scheme 2) of the two possible isomers C-3″ (*S*; **1a**) and C-3″ (*R*; **1b**), leaving all the other stereocenters unaltered (Scheme 1). All three conformations of stereoisomers **1a** and **1b** were optimized at the DFT level by using the B3LYP functional and the 6-31G(d) basis set. On the resulting geometries, the ^{13}C NMR chemical shifts for each stereoisomer were calculated by using the same functional and the 6-31G(d,p) basis (Gaussian 03 Software Package)[27] and by taking into account the Boltzmann-weighted average derived from the energies of the single conformers. The calculated ^{13}C NMR chemical shifts were compared to the experimental ones, showing that the resonances of almost all carbon atoms for both diastereoisomers (**1a** and **1b**) differed by a maximum of 0.2 ppm, except for C-4″ and C-5″. Isomer **1a** presented a predicted C-4″ value of $\delta = 23.1$ ppm, whereas **1b** gave a value of $\delta = 19.7$ ppm. For **1a**, the C-5″ signal was predicted at $\delta = 37.3$ ppm and at $\delta = 40.6$ ppm for **1b** (Table 1). This variation reflects the different magnetic environment for the methyl group in the 4″-position and the methylene group in the 5″-position in **1a** and **1b** due to the different configuration of C-3″. Isomer **1a** showed a variation of 0.7 ppm for C-4″ and C-5″, whereas for **1b** larger $\Delta\delta$ values were found: 2.7 and 4.0 ppm for C-4″ and C-5″, respectively. Moreover, the experimental difference between the chemical shifts of C-4″ and C-5″ was also compared with the corresponding theoretical values for **1a** and **1b**. This comparison was made to cancel out systematic errors of the described methodology, highlighting the high accuracy in reproducing experimental ^{13}C NMR chemical shifts. In fact, the experimental difference of 14.2 ppm was perfectly reproduced for **1a** ($\delta = 14.2$ ppm), whereas the value of 20.9 ppm for **1b** excluded this hypothesis, suggesting the relative configuration of **1a** for bonannione B. It is noteworthy that the applied level of

theory provides high accuracy in reproducing the experimental chemical shifts[9b] of ^{13}C belonging to sp^3 and sp^2 hybridized carbon atoms, as proven by the successful configurational analysis of several natural compounds.[3,8,9b,28]
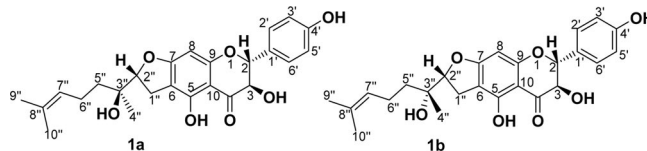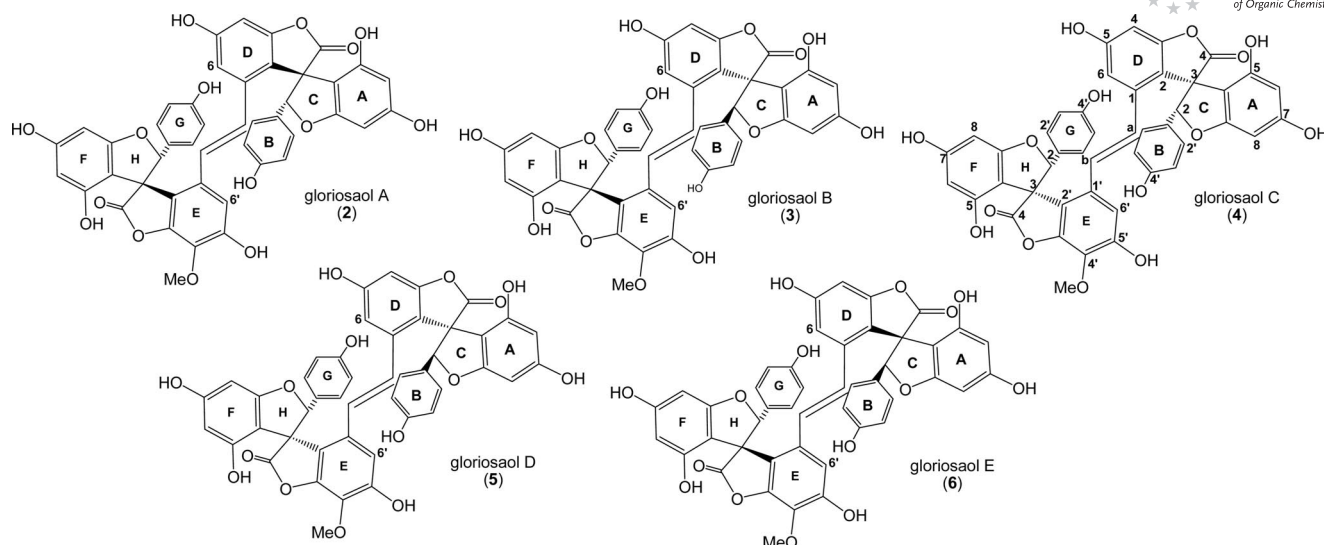

Scheme 1. Molecular structure of **1a** and **1b**.
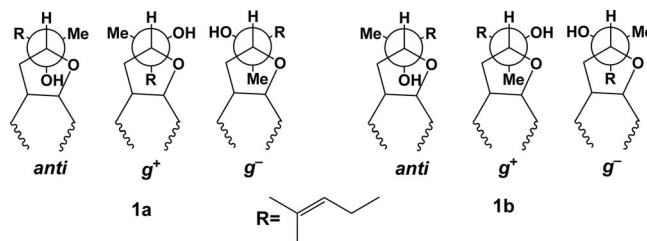
Scheme 2. The *gauche* (g^+ and g^-) and *anti* rotamers around C-2″–C-3″ for compounds **1a** and **1b**. The *gauche* and *anti* position is referred to the –OH group.

Table 1. ^{13}C NMR calculated [B3LYP/6-31G(d,p) level] chemical shifts [ppm] for stereochemical hypotheses **1a** and **1b**, and the ^{13}C NMR experimental data for **1** (600 MHz, CDCl$_3$).

	$\delta(^{13}\text{C})$		
	1a	**1b**	Exp.
2	81.4	81.5	79.0
3	46.2	46.1	42.7
4	187.5	187.5	196.3
5	155.4	155.4	158.3
6	103.2	103.2	105.8
7	161.7	161.7	169.5
8	86.3	86.4	90.5
9	158.4	158.4	163.6
10	101.9	101.9	103.1
1′	127.2	127.2	129.6
2′	122.4	122.5	127.6
3′	107.4	107.4	115.8
4′	150.5	150.5	156.8
5′	111.0	110.9	115.8
6′	123.2	123.3	127.6
1″	29.1	29.5	25.9
2″	94.0	94.0	91.3
3″	73.9	73.9	73.8
4″	23.1	19.7	22.4
5″	37.3	40.6	36.6
6″	24.8	25.0	21.8
7″	122.1	122.5	123.7
8″	128.7	128.0	132.0
9″	26.5	26.4	25.4
10″	17.5	17.6	17.5

2.2 Atropisomer and Configurational Isomer Analysis through MM, NMR, and Quantum Chemical Calculation of ^{1}H NMR Chemical Shifts

Gloriosaols A–E (**2–6**, Scheme 3) are novel antioxidant derivatives isolated from the phenolic fraction root of the plant *Yucca gloriosa* (Agavaceae).[29,30]

Scheme 3. Molecular structure of gloriosaols A–E.

In this case, a strategy based on quantum mechanical calculation of the ^{1}H NMR chemical shifts, in combination with the analysis of the ROE data, was applied for the structural studies of these new phenolic derivatives. The detailed structural analysis of gloriosaols A and B (**2** and **3**, Scheme 3) was complicated by possible atropisomerism. Because the ^{1}H and ^{13}C NMR spectroscopic data for gloriosaols A and B were almost superimposable, and as a result of the lack of any crucial cross-peaks in the ROESY spectrum necessary to determine different structural features, the first step was to clarify whether the compounds were two restricted rotational conformers of a single configurational isomer. To investigate this hypothesis, a combined strategy was applied that was based on the determination of a possible chemical exchange phenomena through NMR and on the quantum mechanical calculation of the potential energy surface of **2** obtained upon variation of the involved dihedral angles (Figure 2) including the atoms (ϕ, $C_{2D}C_{1D}C_\alpha C_\beta$ and ψ, $C_{2'E}C_{1'E}C_\beta C_\alpha$). In particular, a systematic conformational search put in evidence a series of minimum energy conformers separated by small energy barriers (ca. 4.2–4.8 kcal mol^{-1}), whereas the calculated higher rotational barrier was around 6 kcal mol^{-1}. The analogous conformational search performed on diastereoisomer **3**, built upon inversion of configurations at C-2 and C-3 of ring C, showed small energy discrepancies among the minimum energy conformations found for **2**. Moreover, ^{1}H spectra were executed in [D$_6$]DMSO, for each gloriosaol at various temperatures, focusing on H-6$_{ring D}$ and H-6$'_{ring E}$. As can be clearly observed in the two sets of ^{1}H NMR spectra of gloriosaol A (Figure 3), resonances H-6$_{ring D}$ and H-6$'_{ring E}$ showed no significant changes in their chemical shifts over a wide range of temperatures (300–413 K), a finding in contrast with the conformational interconversion hypothesis and with the low-energy barriers suggested by the previous theoretical potential energy surface analysis. In agreement with these experimental observations, a series of ^{1}H 1D spectra of a mixture of gloriosaols A and B, recorded at

different temperatures (300–413 K), still indicated two sets of signals, which finally excluded an atropisomerism phenomenon for gloriosaols A and B. Following these results, compounds **2** and **3** were treated as diastereoisomers and their relative configuration was assigned by using a QM strategy based on the GIAO calculation[12] of ^{1}H NMR chemical shift values at MPW91PW91 level[31] by using the 6-31G-(d,p) basis set.[9b] Such single-point calculations followed a previous geometry refinement performed by using the same functional and the 6-31G-(d) basis set on the previously found minimum energy conformations for diastereoisomers **2** and **3**. Moreover, the ^{1}H calculated values for H-6$_{ring D}$ and H-6$'_{ring E}$, which were the only resonances exhibiting significant variations in the chemical shifts of gloriosaols A and B, were considered as the only diagnostic resonances for the configurational assignment of **2** and **3**. The chemical shift calculated values (Table 2) for H-6$_{ring D}$ and H-6$'_{ring E}$ of **2** were in good agreement with the corresponding experimental values observed for gloriosaol A ($|\Delta\delta|$ of 0.04 and 0.04 ppm), whereas the results obtained for diastereoisomer **3** fit well with the resonances of gloriosaol B ($\Delta\delta$ = 0.00 and 0.03 ppm). Thus, structure **2** was attributed to gloriosaol A and structure **3** to gloriosaol B. Analysis of the 3D structures of **3** (Figure 4) revealed that H-6 and H-6$'$ are directed toward rings F and A, respectively, whereas for **2** these protons probably do not exert CH–π interactions. Thus, H-6 and H-6$'$ are in different chemical and magnetic environments, justifying their chemical shift variations in the structures of gloriosaol A and B. The configurational assignment was further corroborated by analysis of the ROE cross-peaks on the basis of distances measured through careful examination of the calculated structures of the two diastereoisomers.[29] In particular, the distances of 3.31 and 4.50 Å between H-6$'_{ring E}$ and H-2$_{ring C}$ together with the distances of 3.33 and 4.50 Å between H-6$_{ring D}$ and H-2$_{ring H}$ for stereoisomers **2** and **3**, respectively, were in accordance with the presence of two expected cross-peaks observed in the ROESY spectra of

Table 2. Experimental values of H-6$_{\text{ring D}}$ and H-6'$_{\text{ring E}}$ for gloriosaol A and B and calculated values of H-6$_{\text{ring D}}$ and H-6'$_{\text{ring E}}$ for **2** and **3** [δ, ppm]. Comparison, expressed as $\Delta\delta$[a] values, between experimental and calculated chemical shift values.

Atom	Gloriosaol A	**2**	**3**	|$\Delta\delta$| Gloriosaol A – **2**	|$\Delta\delta$| Gloriosaol A – **3**
H-6 (ring D)	6.47	6.43	6.60	0.04	0.13
H-6' (ring E)	6.57	6.53	6.66	0.04	0.09
Atom	Gloriosaol B	**2**	**3**	|$\Delta\delta$| Gloriosaol B – **3**	|$\Delta\delta$| Gloriosaol B – **3**
H-6 (ring D)	6.60	6.43	6.60	0.17	0.00
H-6' (ring E)	6.69	6.53	6.66	0.16	0.03

[a] \|$\Delta\delta$\| = \|$\delta_{\text{exp.}} - \delta_{\text{calcd.}}$\|, absolute difference of the experimental and mean calculated ^{1}H NMR chemical shifts.

gloriosaol A and the absence in the spectra of gloriosaol B. The case studies of **1**–**3** highlight how QM calculation of the ^{1}H/^{13}C NMR chemical shifts are able to probe the different 3D spatial arrangement of stereogenic carbon substituents, suggesting the correct relative configuration of the analyzed compound. Following the approach used for gloriosaols A and B,[29] the relative configurations of gloriosaols C–E were assigned by a combination of NMR analysis and quantum QM methods. In particular, these molecules were apparently not accompanied by their corresponding relative diastereoisomers, so the analysis of atropisomerism was not required. For further details we refer to the original paper.[30]
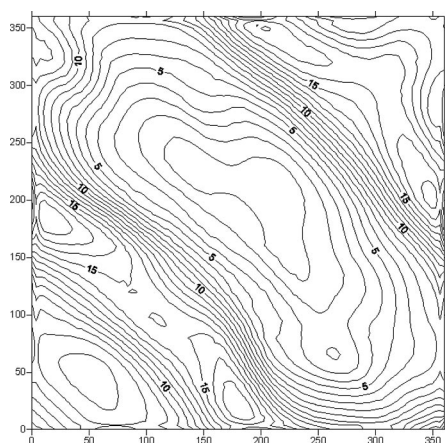

Figure 4. Differences in the spatial arrangements of H-6$_{\text{ring D}}$ and H-6'$_{\text{ring E}}$ of structures **2** and **3**.

2.3 NOE Effects Combined with QM Calculation of ^{13}C NMR Chemical Shifts for the Stereostructural Determination of Aplysqualenol A

Recently, Ishikawa and co-workers[32] applied QM calculation of ^{13}C NMR chemical shifts for the relative configurational assignment of aplysqualenol A (**7**, Scheme 4), extracted from the sea slug *Aplysia dactylomela*. This application, along with the case study of aplysiol B (see section 3.4),[61] shows how the ^{13}C-based approach can be useful for the configurational assignment of an isolated stereocenter belonging to a flexible structural portion. The authors observed a vicinal axial–axial coupling constant of H-3 (12.3 Hz), assigning an equatorial orientation of the bromine atom at C-3 on the A ring (Scheme 4). Moreover, the proton signal for H-14 appeared as a doublet of doublets, suggesting an axial orientation of this methine group. On the basis of these experimental observations, the relative configuration of the A–D rings of **7** was straightforwardly assigned by analysis of the 2D NOESY spectra. Concerning the relative configuration of C-22, Ishikawa and co-workers applied DFT calculations of ^{13}C NMR chemical shifts for all four stereoisomers relative to the couple of atoms C-15 and C-22: 15*R*,22*S*; 15*R*,22*R*; 15*S*,22*R*; 15*S*,22*S*. The comparison of calculated versus experimental chemical shift

Figure 2. Contour plot representations of the potential energy values (kcal mol^{-1}) of gloriosaol A (**2**) vs. ϕ (C$_{\text{2D}}$C$_{\text{1D}}$C$_\alpha$C$_\beta$) and ψ (C$_{\text{2'E}}$C$_{\text{1'E}}$C$_\beta$C$_\alpha$) dihedral angles (°). The map has been obtained by systematic variation of 5° steps of two dihedral angles at empirical (MMFFs force-field) and semiempirical (PM3) levels.
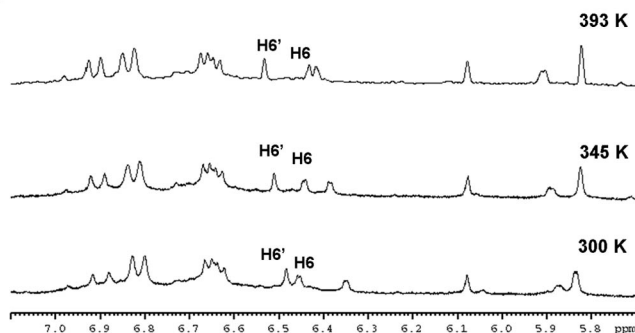

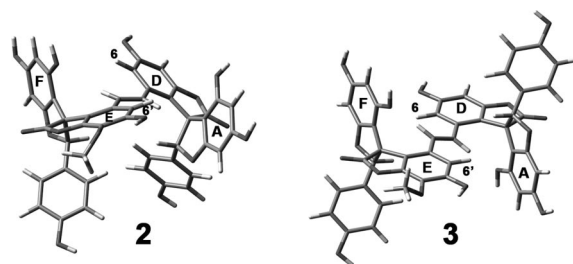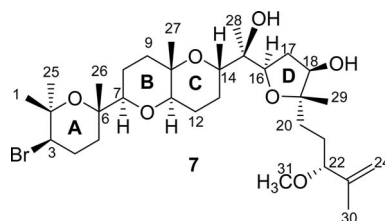Figure 3. Expanded region of [1]H 1D spectra of gloriosaol A.


Scheme 4. Molecular structure of aplysqualenol A (**7**).

values allowed the relative configuration of aplysqualenol A to be assigned as 3*R*,6*S*,7*R*,10*S*,11*R*,14*S*,15*R*,16*R*,18*R*, 19*S*,22*R* (**7**, Scheme 4).

2.4 Configurational Assignment of the New Germacrane Ketopelenolides C and D by NMR and Quantum Chemical Calculation of ^{13}C NMR Chemical Shifts
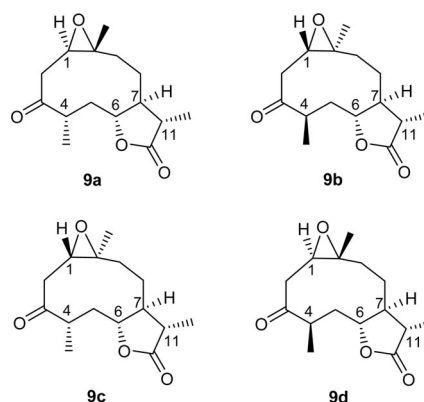
The stereostructural assignment of *Artemisia arborescens* derivatives ketopelenolides C (**8**) and D (**9**, Scheme 5) represent the first evidence for the applicability of the QM GIAO-based computational technique to compounds having nonrigid, medium-sized rings.[33] Even though germacrane derivative ketopelenolide C (**8**) presents five stereogenic carbon atoms, thanks to determination of the absolute configuration of C-1 by a modified Mosher's method[34] and analysis of the NMR spectroscopic data, only four stereoisomers **8a–d** were considered as possible candidates for the configurational assignment (Scheme 6). In this case, the general ^{13}C-based protocol (Figure 1) reported above was applied.[8] For all the four possible stereoisomers, a conformational search by simulated annealing was performed, and the resulting significantly populated conformers of each stereoisomer were ranked in different families: **8a** (5 families), **8b** (7 families), **8c** (5 families), **8d** (7 families). After a step of geometry optimization by semiempirical calculations, the obtained geometries for each family were further optimized at the QM level and then GIAO ^{13}C NMR calculations of all the so-obtained structures were performed. Comparison of the Boltzmann-averaged NMR parameters calculated for each stereoisomer with those experimentally measured for the germacrane derivatives clearly puts in evidence the better fit of **8a** with the experimental values (**8a**$_{MAE}$ = 1.69 ppm, **8b**$_{MAE}$ = 2.2 ppm, **8c**$_{MAE}$ = 1.9 ppm, **8d**$_{MAE}$ = 2.2 ppm; MAE = mean absolute error). The same approach was used for the determination of the stereostructure of ketopelenolide D (**9**, Scheme 5). Also, in this case the assignment obtained by NMR experimental data analysis (*trans* geometry of the epoxide ring) combined with MM/MD was confirmed by GIAO quantum mechanical calculation of ^{13}C NMR chemical shifts. In fact, among the four different stereoisomers [**9a** (5 families), **9b** (7 families), **9c** (4 families), **9d** (5 families) (Scheme 7)] **9a** presented the best agreement with the experimental data (**9a**$_{MAE}$ = 1.4 ppm, **9b**$_{MAE}$ = 1.5 ppm, **9c**$_{MAE}$ = 2.3 ppm, **9d**$_{MAE}$ = 1.8 ppm), and so it was assigned to ketopelenolide D.
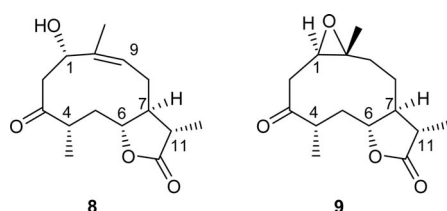
Scheme 5. Molecular structure of ketopelenolide C and D.
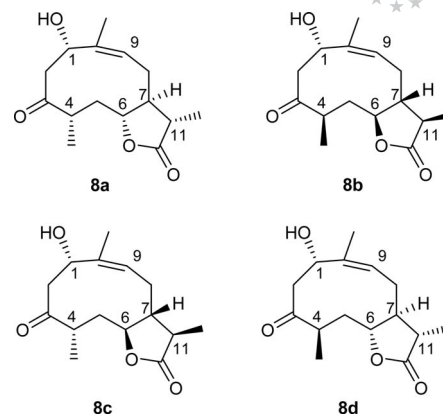

Scheme 6. The four possible stereoisomers of ketopelenolide C.

Scheme 7. The four possible stereoisomers of ketopelenolide D.

2.5 The Pursuit of Stereostructure of Maitotoxin

The stereostructural assignment of the marine neurotoxin maitotoxin was investigated by Nicolaou et al. in 2007.[35] His work regarded the assessment of the relative configuration at the J/K ring junction (C-51/C-52). The question was raised by Gallimore and Spencer[36] in biosynthetic studies, where they hypothesized the inversion of the C-51 and C-52 configuration, confuting the absolute configuration of the overall structure of maitotoxin originally proposed by three different groups: Yasumoto,[37] Tachibana,[38] and Kishi[39] (**10**, Scheme 8). In particular, the absolute configuration of the C136–C142 domain was established by comparison of fragments derived from degradation and synthetic studies. The absolute configuration of the C-136–C-142 domain was used to assign the absolute stereochemistry of the F′E′D′C′B′A′ZYXW domain. This latter information was then used to assign the absolute configuration of the VUTSRQP domain, which was in turn used to assign the absolute configuration of the ONML domain, and on that basis the absolute stereochemistry of the GHIJK domain was derived. Consequently, to check the Gallimore and Spencer hypothesis, Nicolaou et al. performed ^{13}C NMR chemical shift calculations of the simplified maitotoxin skeletons **10a**, **11**, and **12** (Scheme 9), after validation of such methodology to the structure of brevetoxin B,[40] a structural analogue of maitotoxin. Trunc-
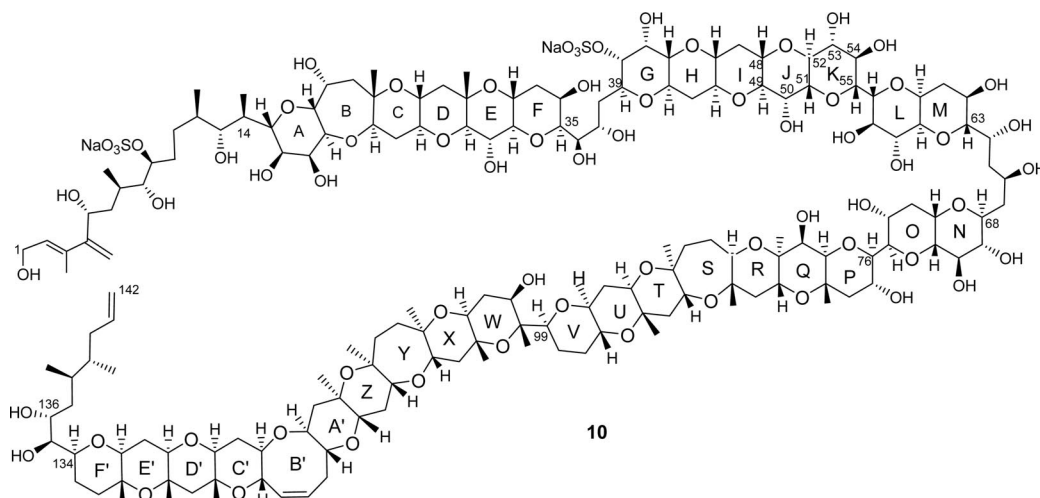
Scheme 8. Molecular structure of maitotoxin proposed by Yasumoto,[37] Tachibana,[38] and Kishi.[39]
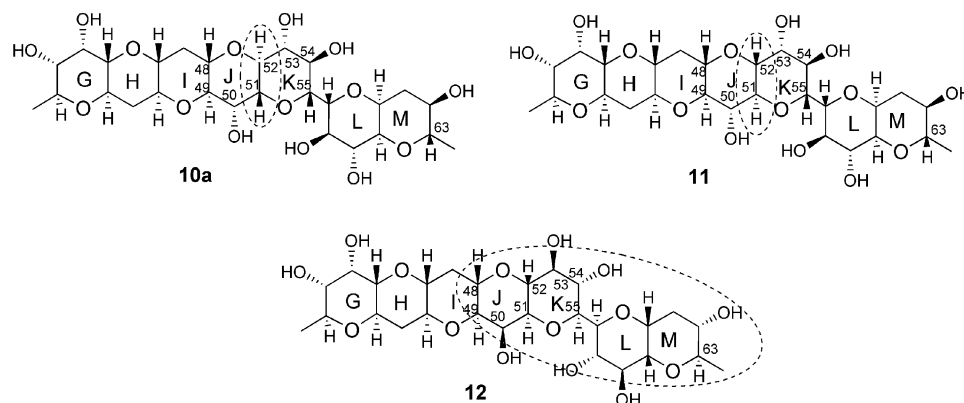

Scheme 9. Three different simplified skeletons of maitotoxin.

ated models **10a**, **11**, and **12** accounted for the three alternative maitotoxin structures under consideration (Scheme 9). In particular, **10a** corresponds to the original structure proposed for maitotoxin,[37–39] **11** correspond to the revised structure only considering the reversion of the J/K ring junction, and **12** corresponds to the revised structure with reversed stereocenters at C-50–C-55. In particular, the last truncated structure was derived from reconsideration of the stereostructural assignment of **10** by considering that the hypothesis of Gallimore and Spencer was correct. From comparison with the experimental NMR spectroscopic data, **10a** likely represents the most correct structure ($\Delta\delta_{10a}$ = 0.78 ppm), followed by **12** ($\Delta\delta_{12}$ = 2.98 ppm) and **11** ($\Delta\delta_{11}$ = 3.03 ppm). In the absence of an X-ray crystal structure of maitotoxin, the real stereostructure can only be confirmed by chemical synthesis, and on the basis of the above accomplished results, Nicolaou et al. suggested the construction of the two truncated GHIJK domains **10a** and **12** as starting points to follow total synthesis studies consistent with their alternative biosynthetic pathway.

2.6 Assignment of Both Natural 6β-Hydroxyhyoscyamine Diastereoisomers by QM Calculation of ¹H and ¹³C NMR Chemical Shifts

On the basis of the great potential offered by GIAO ¹³C and ¹H NMR chemical shift calculations in the determination of relative configuration as reported above, a combined QM–NMR strategy was used to determine the absolute configurations of the diastereoisomers of the tropane alkaloid 6β-hydroxyhyoscyamine.[41] In this work, Muñoz and co-workers present a deepening and re-elaboration of their previous study, where the absolute configurations of the two natural diastereoisomeric forms (3*R*,6*R*,2′*S* **13** and 3*S*,6*S*,2′*S* **14**, Scheme 10) were assigned by using vibrational circular dichroism (VCD) spectroscopy,[42] but some unusual spectroscopic characteristics of these molecules were not completely obvious. For these reasons, they used ¹H and ¹³C NMR chemical shift predictions (GIAO–DFT) to confirm the configuration of both diastereoisomers of 6β-hydroxyhyoscyamine and to explain the differ-

ences observed between their NMR spectra. In particular, it was supposed that the ring current effect of the phenyl group over the tropane bicycle caused rather large differences between these diastereoisomeric species. The previous[42] energetic and geometric data of both diastereoisomers of 6β-hydroxyhyoscyamine were further minimized at the DFT level, and the corresponding chemical shifts were computed and compared with the experimental data of the dextrorotatory and levorotatory stereoisomers. For the ^{1}H NMR predictions, the obtained average absolute differences (Δ_{aa}) and root mean square (rms) errors for each comparison showed that the experimental chemical shifts of dextrorotatory and levorotatory 6β-hydroxyhyoscyamine correlated well with the theoretical values calculated for **13** ($3R,6R,2'S$) and **14** ($3S,6S,2'S$), respectively, whereas for the ^{13}C atoms the calculations were unable to differentiate between the isomers (see Table 3) as already reported for penam β-lactams.[43] This result was underlined by the authors, because calculation of the ^{13}C NMR chemical shifts is usually preferred to the ^{1}H NMR predicted chemical shifts in the configurational assignment. Moreover, considering that conformations with the phenyl group positioned below the tropane bicycle are preferred, and the orientation of this group is similar for **13** and **14**, Muñoz et al. attributed the differences in chemical shifts in both diastereoisomers to the magnetic anisotropy characteristic of aromatic systems.[44] The evaluation of the calculated shielding tensors and the calculated ^{1}H NMR chemical shift changes ($\Delta\delta_M$) strongly suggested that higher levels of anisotropy are observed for the nuclei in the left side of the tropane ring, specifically when the nuclei are closer to the phenyl group.[45] This is confirmed by the larger anisotropy for several protons in both diastereoisomers **13** and **14** (see Table 4) caused by the ring current effect of the phenyl group over the tropane bicycle.
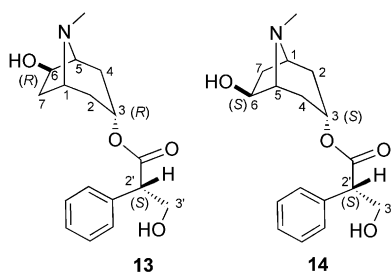
Scheme 10. Structures of diastereoisomers **13**-($3R,6R,2'S$) and **14**-($3S,6S,2'S$) of 6β-hydroxyhyoscyamine.

Table 3. Average absolute differences (Δ_{aa}) and root mean square (rms) errors for comparison between theoretical and experimental chemical shifts of **13** and **14**.

		Dextrorotatory		Levorotatory	
		$3R,6R,2'S$	$3S,6S,2'S$	$3R,6R,2'S$	$3S,6S,2'S$
^{1}H	Δ_{aa}	0.20	0.25	0.28	0.20
	rms	0.23	0.33	0.40	0.23
^{13}C	Δ_{aa}	4.3	4.4	4.4	4.4
	rms	5.3	5.4	5.3	5.4

Table 4. Calculated chemical shift changes ($\Delta\delta_M$) of selected nuclei in the tropane ring of **13** and **14** induced by the benzene ring, and chemical shift differences calculated from these changes [$\Delta\delta_M$(**14**–**13**)] and from experimental chemical shifts ($\Delta\delta_{exp}$) of nuclei with the same chemical environment between **13** and **14**.

	$\Delta\delta_M$**13**	$\Delta\delta_M$**14**	$\Delta\delta_M$(**14**–**13**)	$\Delta\delta_{Exp.}$
1	0.02	0.24	0.22	0.10
2endo	0.02	0.06	0.03	0.07
2exo	0.03	0.27	0.23	0.18
4endo	0.06	0.02	–0.04	–0.10
4exo	0.32	0.04	–0.29	–0.25
5	0.14	0.02	–0.12	–0.15
6	0.34	0.09	–0.25	–0.64
7endo	0.07	2.51	2.44	0.50
7exo	0.04	0.20	0.16	0.15

## 2.7 Stereostructural Assignment of a Pair of Diastereoisomers through Calculation of NMR Chemical Shifts

It is not unusual for a chemist to cope with the assignment of two experimental data sets of two possible diastereoisomers. In a stereoselective synthesis, for example, the reaction gives a small amount of a minor diastereoisomer along with the principal product, and identification of the major compound is a key step in optimizing the reaction yields and/or to proceed with the optimization of the synthesis. Mixtures of diastereoisomers can be isolated from natural sources, as reported for gloriosaols A and B[29] (section 2.2) and for other natural products.[46] Smith and Goodman, through analysis of a set of 28 pairs of diastereoisomers, have tried to verify the ability of QM calculation of NMR chemical shifts to distinguish between diastereomeric structures.[47] The tested compounds involved intermediates like aldols, acetals, and compounds of natural origin. They used the common approach to calculate the ^{1}H and ^{13}C NMR chemical shifts and to compare the calculated values with the experimental data set, assigning the stereostructure on the basis of the best match between the experimental and calculated values. The novelty of their study consists in the introduction of a new parameter, CP3 (comparison parameter), to evaluate the agreement between the calculated and experimental chemical shift values. The new parameter is based on comparing the differences of calculated chemical shifts versus the experimental ones to cancel out systematic errors,[46,48,49] with the consequence that these differences are better reproduced than the chemical shifts themselves. Smith and Goodman, in their systematic analysis of a set of 28 pairs of diastereoisomers, established that the new CP3 parameter, with high confidence, is significantly more reliable in structural assignments than commonly used parameters such as the mean absolute error (MAE) and the correlation coefficient. They also suggest to calculate the probability of the stereostructural determination by using the theorem of Bayes.[47]

# 3. Quantum Mechanical Calculation of *J* Coupling Constants

3.1 First Application of the QM-*J* Method to a "Real" and Complex Case: Determination of the Configuration of Callipeltin A

The determination of configuration of callipeltin A (**15**) by our research group[50] is a particularly interesting application of the QM-*J* method[18] not only because it represented the first application to a real case but also because the structural reassignment was confirmed by total synthesis and spectral correlation of callipeltin A congeners.[51] Initially, for these potent antiviral marine peptides isolated from the sponges *Callipelta* sp.[52,53] and *Latrunculia* sp.,[54] the configuration[52] of nine amino acid residues of callipeltin A was proposed as L-Ala, (2*R*,3*R*,4*S*)-4-amino-7-guanidino-2,3-dihydroxyheptanoic acid (AGDHE), (3*S*,4*R*)-3,4-dimethyl-L-glutamine (diMeGln), L-Thr (two residues), D-Arg, L-Leu, L-*N*MeAla. In 2002,[54] the L-Ala was reassigned as D-Ala, and L-Thr-1 as D-Thr-1. Subsequently, in 2006[51] we reported the determination of the configuration of the unresolved portions of callipeltin A (Scheme 11): the two units (named AGDHE$_{2,3}$ and AGDHE$_{3,4}$) contained in the AGDHE fragment, the two threonine residues (named D-*a*Thr1 and D-*a*Thr2), and the β-OMeTyr amino acid. In particular, the relative and absolute configuration of the β-OMeTyr residue remained unassigned due to the chemical degradation of this residue under acidic hydrolysis conditions; the relative configuration of AGDHE, except for C4, proposed on the basis of homonuclear *J* coupling analysis[52] was not confirmed by subsequent synthetic studies;[55] the presence of two D-*a*Thr residues in neamphamide,[56] a marine peptide that shows high structural homology with **15**, was in disagreement with previous identification as D-*a*Thr1 and L-Thr2.[54] Following our procedure,[18] for a molecule containing more than a single pair of stereocenters, like callipeltin A, each C2 fragment is examined independently from the rest of the whole molecule, comparing the calculated and experimental $^3J_{H,H}$ and $^{2,3}J_{C,H}$ coupling values. According to the above rational, we designed five C2 fragments for callipeltin A, namely, AGDHE$_{2,3}$, AGDHE$_{3,4}$, D-*a*Thr1, D-*a*Thr2, and β-OMeTyr (Scheme 12). For each fragment, three (one *anti* and two *gauche*) staggered arrangements were considered for each of the two *erythro* and *threo* stereochemical series. Subsequently, each arrangement was optimized at the MPW1PW91 level of theory by using the 6-31G(d) basis set and then the calculation of *J* couplings on the optimized geometries was executed by using the same functional and the 6-31G(d,p) basis set.[9b] For both calculation steps, the IEF-PCM solvent continuum model (methanol solvent) was used.[57] In Figure 5, the experimental data sets of *J* values along with all the calculated coupling constants for the various conformational and configurational arrangements of each of the five C2 fragments originating from callipeltin A are reported. It is important to note that for three out of five stereochemical issues (D-*a*Thr1 residue,

AGDHE$_{2,3}$ and AGDHE$_{3,4}$ C$_2$ systems)[58] the correct configurational assignment was obtained by good-to-excellent agreement between calculated and experimental *J* values (see total absolute deviation, TAD, values in Figure 5). Specifically, for the D-*a*Thr1 residue the sum of absolute errors $\Sigma|J_{calcd.} - J_{exp.}|$ of *g*$^-$ *erythro* arrangement was 4.3 Hz, whereas this parameter in all other cases fell in the 11–17 Hz range. For the AGDHE$_{3,4}$ residue, the best agreement between calculated and experimental was found for the *g*$^-$ *threo* arrangement, characterized by a total deviation of only 3.5 Hz (compared to TAD values of 5.9–15.6 Hz for the "wrong" conformers, see Figure 5). Also, for the AGDHE$_{2,3}$ fragment, the *anti erythro* model displayed the lowest TAD value of 4.9 Hz, much below the other deviations (13.0–23.9 Hz). On the other hand, for the D-*a*Thr2 and β-OMeTyr residues, due to very little difference between TAD values of two different arrangements (5.7 vs. 6.2 Hz and 3.2 vs. 3.5 Hz, respectively; see Figure 5), it was only possible to assign the correct configurations thanks to parallel analysis of the ROESY data. In particular, the *g*$^+$ *erythro* arrangement for the D-*a*Thr2 residue was assigned thanks to a strong ROE dipolar effect between the H-2 proton and the methyl group. This observation was also consistent with the small $^3J_{H-2,Me}$ value and, consequently, with a *gauche* relationship between these groups. The presence of a diagnostic ROE cross-peak between the aromatic proton
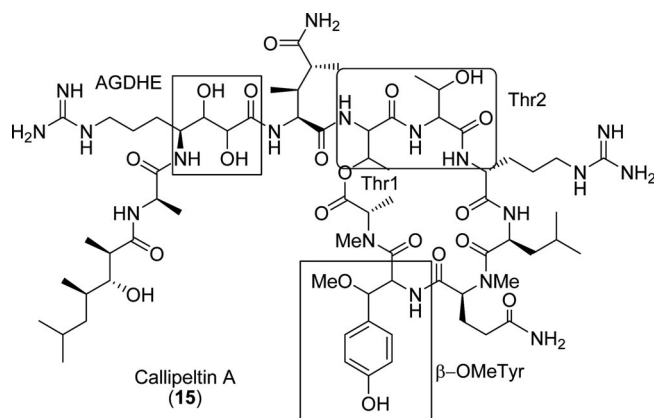
Scheme 11. Callipeltin A (**15**) with amino acid residues still stereochemically undefined.
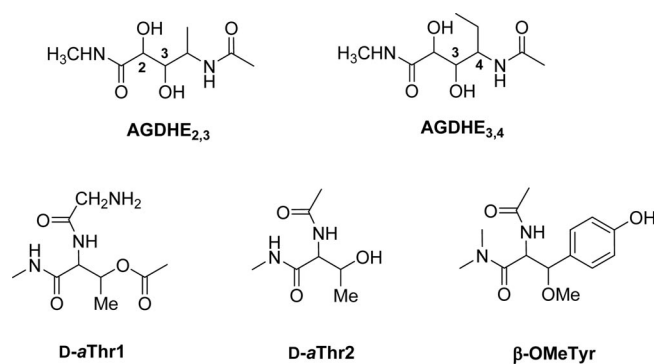
Scheme 12. Molecular fragments representing the five C$_2$ reduced systems of callipeltin A.
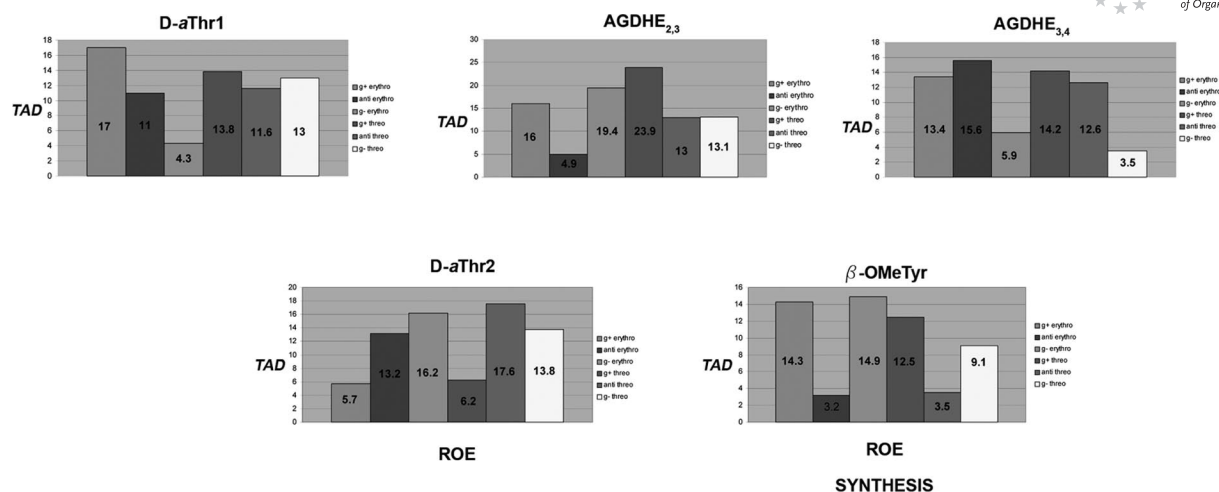
Figure 5. TAD ($\Sigma|J_{calcd.} - J_{exp.}|$) values of callipeltin A for the six conformational arrangements belonging to *erythro* and *threo*.

and the amide proton of the β-OMeTyr residue allowed the *threo* arrangement to be excluded and suggested the *erythro* configuration for the β-OMeTyr residue. These results were confirmed by the synthesis of all four diastereomers of this residue, and the absolute configuration was assigned as 2*R*,3*R* (Scheme 13)[59] and later by the total synthesis of callipeltin B.[51]
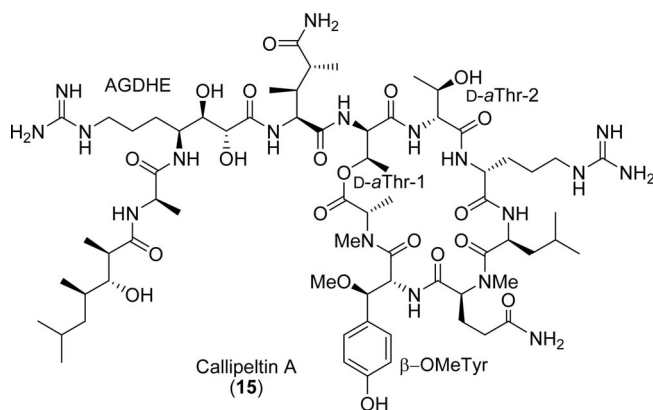

Scheme 13. Revised stereostructure of callipeltin A (**15**).

3.2 Conformational and Configurational Analysis by Calculation of $^3J_{H,H}$ Coupling Constants and NMR Spectroscopy

From the *Bonannia graeca*, besides bonannione B, the flavonoid bonanniol C (**16**) was isolated, and its relative configurational assignment was pursued by a *J*-based approach.[25] In detail, two structural hypothesis were built (**16a** and **16b**, Scheme 14) and their ^{13}C NMR chemical shifts were calculated, but the two sets of Boltzmann-weighted chemical shifts for **16a** and **16b** showed only small differences, not sufficient for a sound assignment of the relative configuration. The next logical step was the application of the *J*-based strategy, not only for its complementarity with the chemical shift calculation approach, but also

for the observation of a set of unusual six-membered ring experimental $^3J_{H,H}$ coupling pattern. In particular, the values of 6.1 Hz for H-2′′/H-1′′β and 5.3 Hz for H-2′′/H-1′′ suggested a possible multiconformational equilibrium. Such observation prompted careful conformational analysis of **16a** and **16b** (Scheme 14), performed by molecular dynamics at different temperatures (400, 600, and 800 K), and for both stereoisomers, two predominant conformers were found (see Figure 6). The following quantum mechanical optimization of the energies and the geometries, performed at the DFT level by using the B3LYP functional and the 6-31G(d) basis set, showed that structure **16a** was represented by two almost equi-energetic conformers (ΔH = 0.022 kcal mol^{-1}), whereas for structure **16b** the slightly larger difference in energy of 0.2 kcal mol^{-1} accounted for a distribution of 60 and 40% for the conformer with the OH group in the axial position and the one with the OH group in equatorial position, respectively. The calculated $^3J_{H,H}$ values [DFT B3LYP and 6-31G(d,p) basis set] of **16a** and **16b**, extrapolated by their Boltzmann-weighted average, were in both cases in good agreement with the experimental values, not allowing a straightforward relative configuration assignment. In fact, for **16a**, the H-2′′/H-1′′β and H-2′′/H-1′′α calculated couplings were 5.7 and 5.3 Hz, respectively, whereas for **16b** calculated values of 5.3 Hz for the H-2′′/H-1′′β coupling and 5.0 Hz for the H-2′′/H-1′′α coupling were observed, resulting in agreement with the equilibrium described above. Consequently, a new set of NMR experiments in methanol were performed with the aim to break the observed hydrogen bond and to induce a conformational equilibrium change for this compound resulting in a $^3J_{H,H}$ value variation. At the theoretical level, the energies and a new set of coupling constants for the conformers of **16a** and **16b** were calculated by simulating the presence of methanol (IEF-PCM) by taking into account the variations in the Boltzmann distribution of the conformers. In particular, the experimental value in CD$_3$OD of the H-2′′/H-1′′β coupling increased to 7.27 Hz and was well reproduced by the hypothetical structure **16a**, with a calculated value of

7.92 Hz. This result is a consequence of the greater contribution of the energetically favored conformer of **16a** having the OH group in the equatorial position, as the reduced weight of the hydrogen bond in CD₃OD for the other conformer was not sufficient to counterbalance the presence of the two bulky axial substituents. On the contrary, the experimental value of 7.27 Hz for the H-2′′/H-1′′β coupling was not well reproduced by the calculated data for **16b**, where no significant variation in the conformations, and therefore in the coupling constants, was observed upon changing the solvent. Careful examination of the 2D ROESY NMR experiments gave the final evidence for the relative configuration of **16a**.[25] In particular, strong dipolar couplings between H-2′′ and H-5′′ and between H-2′′ and H-1′′α and the lack of a strong ROE effect between H-2′′ and Me-4′′ were in agreement with the H-2′′α arrangement depicted in **16a**.
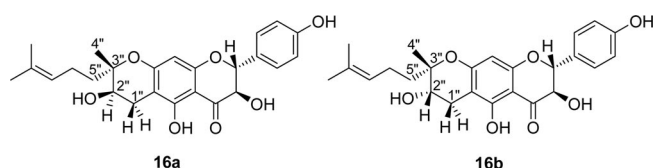
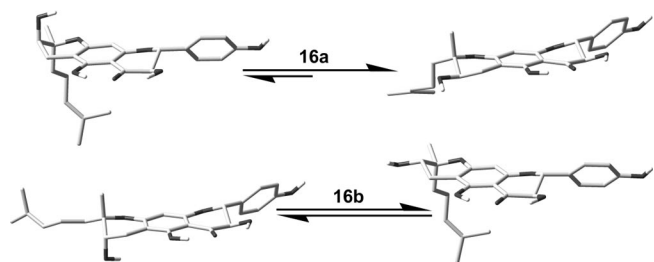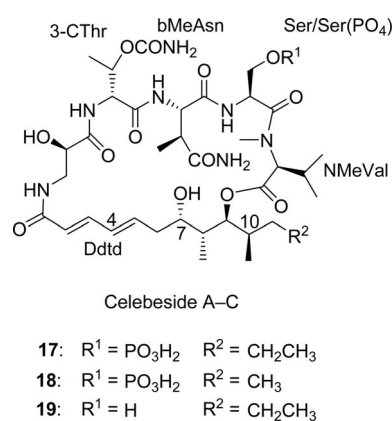Scheme 14. Molecular structure of **16a** and **16b**.

Figure 6. Conformational equilibrium for stereoisomers **16a** and **16b**. For both stereoisomers, one conformer presents the OH group at C-2′′ in the equatorial position, and the other is characterized by the axial position of the hydroxy group, which is balanced by the presence of a hydrogen bond with the oxygen atom at C-3′′.

3.3. *J*-Based Configurational Analysis Vs. QM Calculation of ³$J_{H,H}$ and ²,³$J_{C,H}$ Coupling Constants

Celebesides A–C (Scheme 15) were isolated from the marine sponge *Siliquariaspongia mirabilis*.[60] They are cyclic depsipeptides that comprise a polyketide moiety (Ddtd), whose relative configurations of the stereogenic centers C-7, C-8, and C-9 were determined by quantum mechanical calculation of the homonuclear and heteronuclear *J*-coupling values. In particular, the celebesides are here reported as an example of configurational assignments of stereocenters that are members of flexible macrocycles, highlighting some drawbacks of the *J*-based approach proposed by Murata.[6] The first attempt to assign the relative configuration of the stereocenters was made by applying the protocol of

Murata.[6] Because some ³$J_{C,H}$ experimental values were not easily classifiable as small or large, qualitative analysis could have led to wrong configurational assignment. For this reason, the relative configuration was studied by using the same quantitative QM/NMR strategy[18] adopted for callipeltin A: DFT MPW1PW91/6-31G(d,p) calculations of *J* values (Table 5) for all possible configurations in the simplified fragment **A** (Scheme 16). The quantitative approach is very helpful when experimental coupling constants fall out of the ranges qualitatively classified as "large" or "small", especially for ²,³$J_{C,H}$. presenting a smaller range (0 to 6 Hz) of coupling constant values than the relatively larger range (0–12 Hz) of ³$J_{H,H}$ values. As an example, the experimental ³$J_{C,H}$ values for H-7/C-9, H-8/C-6, and H-9/C-11 within the Ddtd portion of **17** were found to be 3.1, 2.6, and 4.0 Hz, respectively, all of which may be classified as "medium". Analysis of the compared experimental and calculated *J* coupling constants displayed the isomers A3


Scheme 15. Molecular structure of celebesides A–C (**17–19**).

Table 5. Calculated and experimental *J* values for a fragment corresponding to Ddtd in celebeside A (**17**).

C7–C8	A1	A2	A3	A4	A5	A6	Exp.
	threo			*erythro*			
H7,Me8	2.7	4.0	4.3	2.9	4.2	5.1	5.5
H7,C9	4.9	0.4	2.1	5.6	1.5	0.1	3.1
H8,C6	4.4	1.7	0.5	0.7	5.2	5.7	2.6
H8,H7	2.7	7.5	2.2	2.4	4.1	6.3	1
TAD[a]	8.0	11.7	5.5	8.4	8.7	11.8	
C8–C9	B1	B2	B3	B4	B5	B6	
H8,C9	–0.4	–4.8	–3.8	–4.1	–0.7	–5.2	–7.2
H9,C7	5.2	5.5	1.8	2.3	2.3	1.2	3.0
H9,Me8	1.5	3.6	2.7	1.0	6.5	5.1	1.3
H9,H8	2.0	2.5	9.0	9.2	1.2	5.1	10.6
TAD[a]	17.8	15.3	7.6	5.5	21.9	13.0	
C9–C10	C1	C2	C3	C4	C5	C6	
H9,Me10	5.0	0.4	2.5	6.6	4.7	2.9	5.3
H9,C11	2.6	6.2	4.4	0.3	2.2	4.7	4.0
H10,C9	2.3	–2.0	–5.7	–2.1	–5.7	2.3	1.3
H10,H9	2.6	4.4	2.4	4.8	2.3	2.7	1.1
TAD[a]	4.2	13.7	11.3	12.1	10.7	5.7	

[a] Total absolute deviation (Σ|$J_{calcd.}$ – $J_{exp.}$|) values.

for C-7/C-8 (5.5 Hz), B4 for C-8/C-9 (5.5 Hz), and C1 for C-9/C10 (4.2 Hz), as presenting the lowest total absolute deviation (TAD, Table 5) values confirming the J-based relative configuration presented above. In detail, the obtained configuration for the structural portion examined was $7S,8R,9S,10R$. Moreover, the experimental ROESY correlations (Figure 7) were perfectly compatible with the results outlined by J coupling quantum chemical analysis.[60]
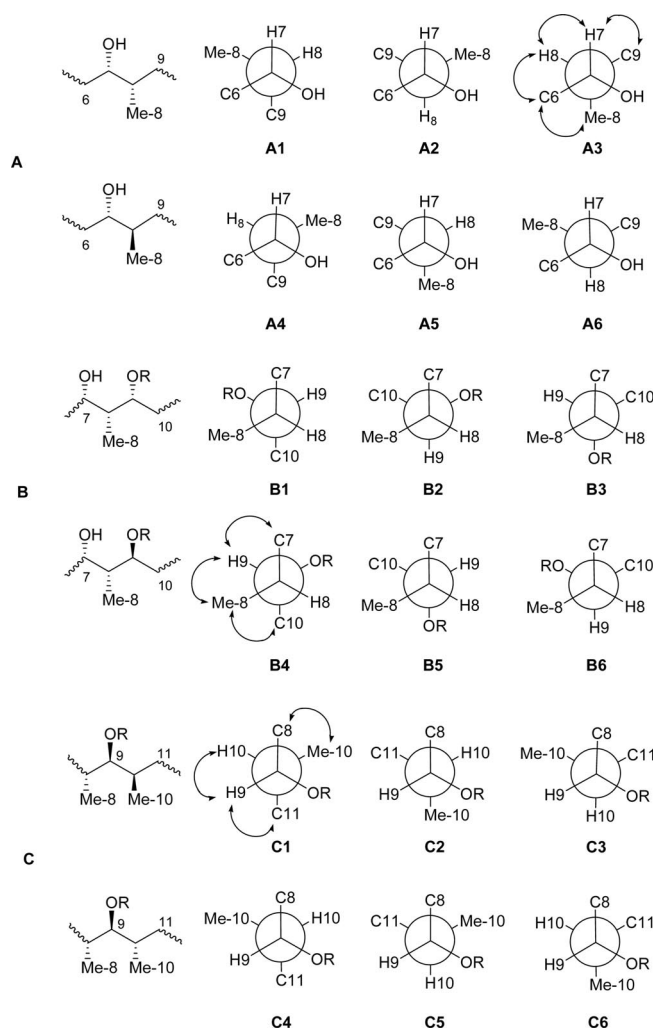
Scheme 16. Newman projections showing all possible staggered rotamers for *threo* and *erythro* configurations viewed down bonds (A) C-7–C-8, (B) C-8–C-9, and (C) C-9–C-10 for the polyketide residue Ddtd in compound **17**.
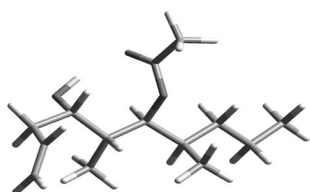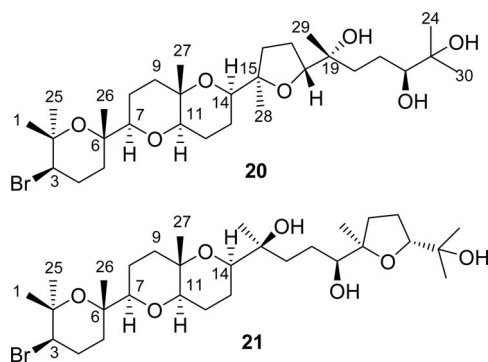

Figure 7. DFT MPW1PW91/6-31G(d,p) geometry and energy-optimized conformer of the C-4 to C-12 fragment of Ddtd in **17**–**19**.

## 3.4. Stereochemical Analysis of Aplysiol B through QM–NMR Investigations

The bioactive secondary metabolite aplysiol B (**20**, Scheme 17) was isolated from the marine organism *Aplysia dactylomela*.[61] The case study of aplysiol B is an interesting example of integration between different experimental techniques of NMR spectroscopy and quantum chemical calculation of NMR parameters. The strategy adopted here for the configurational assignment of the five stereogenic centers includes the QM calculations of ^{13}C and $^{2,3}J_{C,H}$ and $^3J_{H,H}$ coupling constants along with the supporting analysis of 2D ROESY data, showing that for the investigation of stereocenter couples, even within a single organic compound, the choice method has to be determined after careful examination of the data and may differ from one to the other couple of stereocenters.[61] As an example, the configuration of the tetrahydrofuran ring was obtained by straightforward experimental analysis of ROE cross-peaks. Compound **20** is biogenetically correlated to thyrsiferol (**21**, Scheme 17), whose absolute configuration was determined by stereospecific synthesis.[62] Moreover, aplysiol B (**20**) and thyrsiferol (**21**) have an identical, rigid, left-side moiety as shown by superimposable ^1H and ^{13}C NMR chemical shift values, and the relative configuration of the left-side moiety was also confirmed by ROESY experiments.[63] In the structural analysis of aplysiol B, the absolute configuration of the common rigid left-side moiety was kept and used as a reference point for the stereochemical establishment of **20**. Following the strategy based on the QM calculation of J couplings for the determination of the relative configuration of adjacent couple of stereocenters,[18] the arrangement of the C_2 fragments C-14/C-15 and C-18/C-19 were examined by using two simplified molecular fragments[18] of the entire molecule (Scheme 18). Such fragments were considered by taking into account the two possible diastereomers *erythro* and *threo*, and all the three staggered rotamers (g^+, g^-, and *anti*) for each stereoisomer (Table 6). In particular, although in the original paper[18] it is proposed to substitute the main chain by at least two heavy groups (carbon, oxygen atoms) and every branched chain by at least one heavy atom, in our case for both fragments C-14/C-15 and C-18/C-19 some of the stereogenic carbons were part of a cycle; for this reason the complete ring portion containing the stereogenic atoms was included in the calculations,[61] going well over the lowest requirements suggested in the original paper.[18] For the C-14/C-15 fragment, the calculated J values for two of the six arrangements, namely, the *anti threo* and the *anti erythro*, were in good agreement with the experimental ones, by showing the lowest sum of absolute errors $\Sigma|J_{calcd.} - J_{exp.}|$ (total absolute deviation values, TAD) in the reproduction of J experimental data; it is noteworthy that for such arrangements, all the single J calculated values differ from the experimental ones by less than 1 Hz. The quantitative investigation of the calculated versus the experimental data allowed a slightly better agreement for the *anti threo* arrangement to be observed (Table 6). A complementary confirmation of the *anti threo* arrangement came from

the analysis of the ROESY data, revealing crucial dipolar correlations between H-14 and H$_3$-23 and H-16α, and between H$_3$-23 and H-13. On the basis of the knowledge of the absolute configuration of C-14 (derived from the established configuration of **21**), the *R,R* configuration of the C-14/C-15 fragment was assigned. The analysis of the C2 fragment C-18/C-19 (see Table 6) revealed that only the *g*$^+$ rotamer of the *threo* arrangement was in good agreement with the experimental *J* values, presenting differences between calculated and experimental data lower than 1 Hz, despite all the other rotamers. The presence of dipolar couplings between H-18 and H$_3$-29 and H$_2$-20, and between H-17 and H$_2$-20 confirmed the QM *J*-based results, allowing the *threo* configuration for the fragment C-18/C-19 to be assigned. To determine the configuration of the tetrahydrofuran ring, and thus the relationship between C-15 and C-18, careful examination of the 2D ROESY data was carried out. In particular, the strong dipolar couplings between H-14 and H$_3$-28 and H-16α (Figure 8), between H-16β and H$_3$-28, and between H-18 and H-16α allowed the *R* absolute configuration of C-18 to be established and, following the information derived from the above *J*-based analysis, the consequent *R* configuration for C-19. Once obtained, the 14*R*,15*R*,18*R*,19*R* configuration, the isolated C-22 stereocenter was analyzed by building two possible models **20** and **22** (Scheme 19), having the 14*R*,15*R*,18*R*,19*R*,22*S* and the 14*R*,15*R*,18*R*,19*R*,22*R* configuration, respectively. For such models the ^{13}C NMR chemical shifts at the quantum mechanical level were calculated and subsequently compared with the experimental data.[8] In detail, conformational search of the two models by molecular mechanics (MonteCarlo multiple minimum method of the MacroModel package)[64] was performed. All the significant conformers of the two diastereoisomers were subsequently optimized at the DFT level by using the MPW1PW91 functional and the 6-31G(d) basis set. On the so-obtained geometries, single-point calculation of the ^{13}C NMR chemical shifts were performed by using the same functional and the 6-31G(d,p) basis set; the final chemical shift values for each diastereoisomer was derived by taking into account the Boltzmann-weighted average based on the energies of the single conformers for each stereoisomer. The

resulting ^{13}C NMR chemical shifts corresponding to models **20** and **22** were compared with the experimental ones (Table 7, together with the mean absolute errors, MAE, for
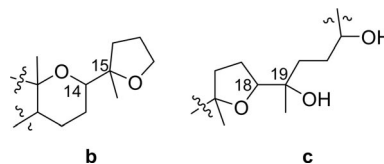
Scheme 18. Molecular fragments **b** and **c** representing the reduced systems of **20** including the portions C-14/C-15 and C-18/C-19, respectively.

Table 6. Calculated [MPW1PW91/6-31G(d,p) level] $^{2,3}J_{C,H}$ coupling constants of aplysiol B (**20**) for the six conformational arrangements belonging to the *erythro* and *threo* series in comparison with the experimental data: single deviations and TAD ($\Sigma|J_{calcd.} - J_{exp.}|$) values.

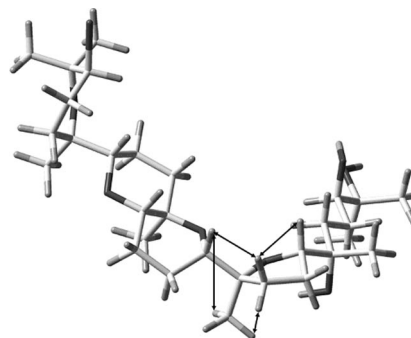|	Calcd.						Exp.
		eythro			*threo*		
	g$^+$	*anti*	*g*$^-$	*g*$^+$	*anti*	*g*$^-$	
b (C14–C15)							
$^2J_{C15,H14}$	–3.1	1.5	–1.8	–3.1	2.3	–2.1	2.3
$^3J_{C16,H14}$	2.7	1.1	2.6	1.2	0.6	3.0	0.9
$^3J_{Me,H14}$	1.8	0.7	2.9	2.9	1.3	3.1	0.3
TAD	8.7	1.4	8.3	8.2	1.3	9.2	
c (C18–C19)							
$^2J_{C19,H18}$	–0.8	0.3	5.2	–0.1	5.5	–0.2	0.8
$^3J_{C20,H18}$	2.5	3.4	0.8	1.5	1.2	3.8	0.6
$^3J_{Me,H18}$	2.1	2.9	1.4	2.5	0.9	4.6	2.5
TAD	3.9	5.7	3.8	1.9	6.8	6.4	

Figure 8. Significant experimental ROEs (black arrows) for the assignment of the configuration at C-15 and C-18 of **20**.

Scheme 17. Molecular structure of aplysiol B (**20**) and thyrsiferol (**21**).
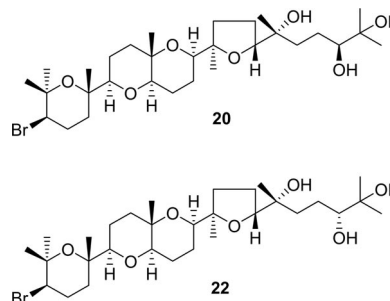
Scheme 19. Two stereoisomers models, **20** and **22**, considered for quantum mechanical calculation of ^{13}C NMR chemical shifts.

each stereoisomer). As shown in Table 7, **20** shows a MAE value of 2.56 vs. 2.84 of **22**, suggesting the *S* configuration for C-22. It is noteworthy that the MAE value of 2.56 is in good agreement with the MAE value of 2.48, obtained at

Table 7. Significant ^{13}C calculated [MPW1PW91/6-31G(d,p) level] chemical shifts [ppm] for **20** and **22**, and corresponding ^{13}C NMR experimental data for aplysiol B.

	δ(^{13}C)		
	Calcd.		Exp.
	20	**22**	
12	26.6	26.7	21.3
13	25.7	26.2	21.4
14	78.1	76.5	75.4
15	82.7	82.9	84.3
18	86.4	87.7	86.4
17	28.3	27.9	25.9
16	35.1	33.9	35.8
28	28.5	26.4	23.2
19	73.2	70.0	72.3
29	19.8	22.2	21.6
20	34.4	40.1	33.7
21	27.4	28.4	25.4
22	72.5	74.6	78.4
23	70.9	70.6	73.1
MAE[a]	2.56	2.84	

[a] Mean absolute error (MAE) found for ^{13}C NMR chemical shifts of compounds **20** and **22** vs. ^{13}C NMR experimental values: MAE = $\Sigma[|(\delta_{exp.} - \delta_{calcd.})|]/n$.

the same level of theory for a set of known natural compounds;[9b] for this reason, such a result not only provides information on the *S* configuration of C-22, but also corroborates the configurational arrangement of C-14, C-15, C-18, and C-19 depicted in **20** and determined as described above. A further contribution to this stereochemical analysis was provided by application of the Mosher method[26] for stereocenter C-22 finally confirming the absolute configuration proposed.

### 3.5. Stereochemical Assignment of 3β,7-Dihydroxy-5,6-epoxycholestanes

The above-described quantitative QM–NMR strategy[18] was successfully applied by several other groups for the elucidation of the relative configuration of some natural and nonnatural products. Among them, Rodrìguez[65] et al. in 2008 determined the correct stereostructural dispositions of the epoxy and hydroxy groups of the four cholesterol derivatives 3β,7-dihydroxy-5,6-epoxycholestanes. The 5,6-epoxy moiety is a key intermediate in the synthesis of active steroids, and so knowledge of the correct stereochemical assignment of this portion is crucial in the subsequent reaction steps. For this reason the authors synthesized four possible diastereoisomers of 3β,7-dihydroxy-5,6-epoxycholestane (**23–26**, Scheme 20). After a preliminary step for the construction of models [conformational search (PCModel package), geometry optimization (DFT/B3LYP/6-31 or 6-

Table 8. Comparison between experimental and calculated $^3J_{H,H}$ and $^2J_{C,H}$ values [Hz] of stereoisomers **23–26**.

	$\Delta^{exp.\alpha\alpha-DFT\alpha\alpha}$	$\Delta^{exp.\alpha\alpha-DFT\alpha\beta}$	$\Delta^{exp.\alpha\alpha-DFT\alpha\beta}$	$\Delta^{exp.\alpha\alpha-DFT\beta\beta}$		$\Delta^{exp.\beta\alpha-DFT\alpha\alpha}$	$\Delta^{exp.\beta\alpha-DFT\alpha\beta}$	$\Delta^{exp.\beta\alpha-DFT\alpha\beta}$	$\Delta^{exp.\beta\alpha-DFT\beta\beta}$
$^3J_{H6,H7}$	0.0	2.1	4.2	2.5	$^3J_{H6,H7}$	2.0	0.1	2.2	0.5
$^3J_{H7,H8}$	0.8	1.5	1.2	2.3	$^3J_{H7,H8}$	2.8	0.5	3.2	4.3
$^2J_{C5,H4a}$	0.3	5.7	0.5	5.8	$^2J_{C5,H4a}$	6.7	1.3	6.5	1.2
$^2J_{C5,H6}$	1.1	1.2	1.6	1.1	$^2J_{C5,H6}$	0.6	0.7	1.1	0.6
$^3J_{C5,H19}$	0.1	1.3	0.1	1.3	$^3J_{C5,H7}$	6.4	2.1	1.2	6.9
$^2J_{C6,H7}$	0.1	2.1	4.2	1.1	$^2J_{C6,H7}$	4.6	2.6	0.5	5.8
$^3J_{C6,H8}$	2.8	2.4	2.6	1.9	$^2J_{C7,H6}$	1.3	1.0	0.7	0.0
$^2J_{C7,H6}$	0.0	0.3	2.0	1.3	$^2J_{C7,H8}$	1.1	0.5	4.9	4.0
$^2J_{C7,H8}$	3.3	2.7	2.7	1.8	$^3J_{C8,H6}$	0.1	0.5	0.7	0.4
$^3J_{C8,H6}$	0.2	0.8	1.0	0.7	$^3J_{C9,H7}$	0.0	1.5	5.6	5.3
Σ	8.7	20.0	20.2	19.7	Σ	25.6	10.8	26.6	29.0
MAD[a]	0.9	2.0	2.0	2.0	MAD[a]	2.6	1.1	2.7	2.9

	$\Delta^{exp.\alpha\beta-DFT\alpha\alpha}$	$\Delta^{exp.\alpha\beta-DFT\alpha\beta}$	$\Delta^{exp.\alpha\beta-DFT\alpha\beta}$	$\Delta^{exp.\alpha\beta-DFT\beta\beta}$		$\Delta^{exp.\beta\beta-DFT\alpha\alpha}$	$\Delta^{exp.\beta\beta-DFT\alpha\beta}$	$\Delta^{exp.\beta\beta-DFT\alpha\beta}$	$\Delta^{exp.\beta\beta-DFT\beta\beta}$
$^3J_{H6,H7}$	4.8	2.7	0.0	2.3	$^3J_{H6,H7}$	3.3	1.2	0.9	0.8
$^3J_{H7,H8}$	0.7	3.0	0.3	0.8	$^3J_{H7,H8}$	2.4	4.7	2.0	0.9
$^2J_{C5,H4a}$	0.2	5.2	0.0	5.3	$^2J_{C5,H4a}$	6.4	1.0	6.2	0.9
$^2J_{C5,H6}$	1.0	0.9	0.5	1.1	$^2J_{C5,H6}$	0.6	0.7	1.1	0.6
$^3J_{C5,H7}$	5.4	1.1	0.2	5.9	$^2J_{C6,H7}$	2.1	0.1	2.0	3.3
$^3J_{C5,H19}$	0.0	1.4	0.0	1.4	$^3J_{C6,H19}$	4.1	4.0	4.3	3.7
$^2J_{C6,H7}$	5.8	3.8	1.7	7.0	$^2J_{C7,H6}$	1.6	1.3	0.4	0.3
$^2J_{C7,H6}$	0.6	0.3	1.4	0.7	$^2J_{C7,H8}$	6.0	5.4	0.0	0.9
$^2J_{C7,H8}$	6.0	5.4	0.0	0.9	$^3J_{C8,H6}$	0.3	0.9	1.1	0.8
$^3J_{C8,H6}$	0.3	0.3	0.5	0.2	$^3J_{C7,H9}$	1.5	1.0	2.1	0.3
$^3J_{C9,H7}$	5.3	3.7	0.4	0.1	Σ	28.2	20.3	20.0	12.4
$^3J_{C14,H7}$	5.9	5.0	1.2	2.5	MAD[a]	2.8	2.0	2.0	1.2
Σ	35.9	32.6	6.2	28.0					
MAD[a]	3.0	2.7	0.5	2.3					

[a] Mean absolute error deviation (MAD) {defined as $\Sigma[(^nJ_{C,H/H,H}$experimental $- ^nJ_{C,H/H,H}$calculated$)/$number of comparisons]}.

311G(d)-Gaussian 03)], the authors easily identified through calculation of coupling constants at the DFT/ MPW1PW91/6-311G(d,p) level the correct configurational assignment on the basis of the mean absolute error deviation (MAD) {defined as $\Sigma[(^{n}J_{\text{CH}_{\text{exp.}}} - ^{n}J_{\text{CH}_{\text{calcd.}}})/\text{number of comparisons}]$}. The calculated data for each model fit better with only one experimental J homo- and heteronuclear data set (see Table 8). Moreover, these results were consistent with the results obtained by GIAO ^{13}C NMR chemical shift calculations. In conclusion, Rodriguez et al. easily discriminated the four different stereoisomers through quantitative MAD parameters, confirming QM–NMR parameter calculations as a powerful tool for the identification of diastereoisomers.
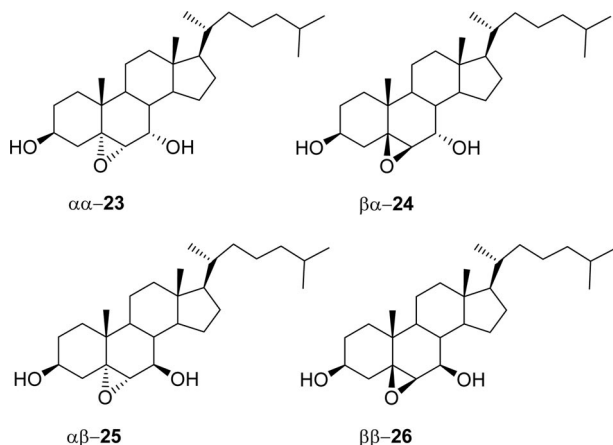

Scheme 20. Molecular structure of four possible 3β,7-dihydroxy-5,6-epoxycholestane diastereoisomers (**23**–**26**).

3.6. Determination of Relative Configuration in Acyclic 1,3-Nitrogen-Containing Moieties

Noncanonical amino acids have been frequently found as structural constituents of natural products and have also been used as nonnatural synthetic amino acids as antimetabolites. Thus, it is very important to have a reliable methodology to determinate the relative configuration of acyclic compounds. The method of Murata could be a tool for structural analysis, but most of the reported molecules studied by the J-based approach usually only contain oxygenated alkyl-substituted compounds. Also, only few compounds with nitrogen-substituted acyclic systems have been reported, and for this reason Rodrìguez et al.[66] highlighted the need to obtain a new set of values to build up reliable curves, which may describe angular dependence versus heteronuclear coupling constants. In a recent contribution, Rodrìguez et al. reported a new structure of the polychlorinated dipeptide dysithiazolamide (**27**, Scheme 21), isolated from the sponge *Dysidea* sp.[67d] The relative configuration of the acyclic moiety of **27** was proposed through J-based analysis on new amino acid derivative **28**, which was used as a model for the stereostructural assignment of the natural product. In subsequent work, the authors, in order to complete the study of J-configurational assignments for 1,3-ni-

trogen-containing acyclic moieties, reported the synthesis of the epimer of **28**, (2S,4R)-dichloroleucine (**27**, Scheme 21) and the corresponding configurational analysis carried out by the J-based method along with QM calculations of chemical shifts. This work is noteworthy because it represents one of the few[18,67] applications of the J-based approach on nitrogen-substituted acyclic systems. Rodrìguez et al., following the J-based method, found for structure **29** the presence of two main conformers in fast interconversion around the bonds C-2/C-3 and C-3/C-4 (Tables 9 and 10). In detail, the observation of medium/large $^{3}J_{\text{H,H}}$ values around the C-2/C-3 (6.3 and 8.4 Hz) and C-3/C-4 (6.5 and 6.4 Hz) bonds suggested a conformational equilibrium. Moreover, for C-2/C-3, the medium values found for $^{3}J_{\text{C1,H3a}}$ and $^{2}J_{\text{C2,H3b}}$ indicated an equilibrium between the *anti* and the *gauche* (–) conformers, where the population of the first one should be higher than that of the second one. The homonuclear coupling constants measured at low temperature showed that the population of the *anti* conformer increased, whereas that of the *gauche* conformer (–) decreased. Similarly, the observation of the intermediate values found for $^{3}J_{\text{Me,H3b}}$, along with the large one for $^{2}J_{\text{C4,H3a}}$ and the small one for $^{3}J_{\text{Me,H3a}}$, suggested the presence of a more complex equilibrium, confirmed also by NMR experiments at low temperature. In a second step, the DFT calculations of ^{1}H and ^{13}C NMR chemical shifts were performed for the six possible staggered rotamers around the C-2/C-3 and C-3/C-4 bonds of **28** and **29**. Analysis of calculated resonances confirmed the presence of a conformational equilibrium found by the investigation of experimental J couplings constants. A combination of the predicted and experimental coupling constants suggested the *syn* configuration for compound **29**.
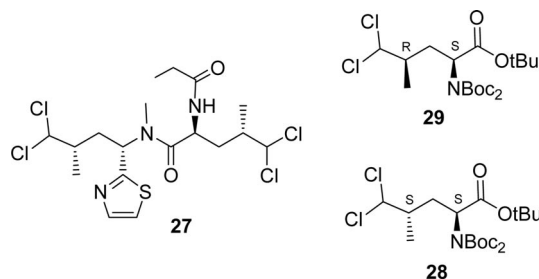
Scheme 21. Molecular structure of polychlorinated dipeptide dysithiazolamide (**27**) and *anti* (**28**) and *syn* (**29**) 5,5-dichloroleucine derivatives.

In this paper, the authors assessed the difficulty to classify the J values for these types of structural systems. In particular, it is important to note that the heteronuclear coupling constant are not only dependent on the dihedral angles but also on other factors such as the electronegativity of the substituents and the presence of hydrogen bonds. Thus, the presence of electronegative atoms could cause $^{2,3}J_{\text{C,H}}$ values to diverge from the values predicted by a simple Karplus equation. The application of DFT calculations to this case study highlights the ability of QM calculations

Table 9. $^3J_{H,H}$ and $^{2,3}J_{C,H}$ values [Hz] around the C-2/C-3 bond for epimers **28** (*anti*) and **29** (*syn*) and comparison with the predicted values for the six possible staggered rotamers for each bond.
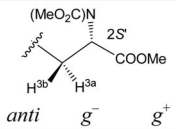
C-2–C-3 bond	Calcd.						Exp.	
	(MeO₂C)N 2S'			(MeO₂C)N 2R'			*anti*	*syn*
	anti	g^-	g^+	*anti*	g^-	g^+		
$^3J_{H2,H3b}$	11.3	3.6	1.8	4.8	4.5	6.5	11.0	6.3 5.9 5.8
$^3J_{H2,H3a}$	3.5	4.9	9.8	11.1	1.7	2.6	4.3	8.4 8.5 8.6
$^3J_{C1,H3b}$	2.4	1.1	7.3	0.4	0.8	8.6	2.4	1.9
$^3J_{C1,H3a}$	0.8	8.7	4.7	2.8	2.2	1.4	0.8	3.5
$^3J_{C4,H2}$	2.1	7.4	3.9	1.3	5.5	6.3	2.8	1.7 1.8
$^2J_{C2,H3b}$	–6.5	–2.1	–4.8	–0.6	–3.4	–2.7	–6.9	–3.6 –3.7
$^2J_{C2,H3a}$	–1.3	–4.0	–5.5	–6.2	–3.3	0.3	–2.5	–6.0 –5.9
MAD 29	2.98	3.09	2.37	1.40	2.48	3.77		
MAD 28	**0.49**	4.01	4.25	4.07	2.73	3.36		

Table 10. $^3J_{H,H}$ and $^{2,3}J_{C,H}$ values [Hz] around the C-3/C-4 bond for epimers **28** (*anti*) and **29** (*syn*), and comparison with the predicted values for the six possible staggered rotamers for each bond.
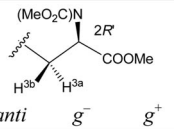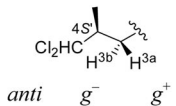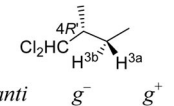
C-3–C-4 bond	Calcd.						Exp.	
	Cl₂HC 4S'			Cl₂HC 4R'			*anti*	*syn*
	anti	g^-	g^+	*anti*	g^-	g^+		
$^3J_{H4,H3b}$	2.2	2.7	9.9	8.5	2.6	3.6	3.0	6.5 7.0 7.0
$^3J_{H4,H3a}$	10.3	5.8	5.2	0.8	1.8	4.0	11.0	6.4 5.6 5.3
$^3J_{C5,H3b}$	1.9	11.2	1.4	0.0	11.6	2.6	3.4	4.7
$^3J_{C5,H3a}$	3.9	0.8	12.3	7.5	3.3	14.1	3.2	6.8
$^3J_{Me,H3b}$	7.0	3.2	3.6	5.3	3.0	2.8	6.2	3.9 4.0
$^3J_{Me,H3a}$	3.4	7.4	1.5	5.6	1.6	7.4	3.0	3.5 3.7
$^3J_{H4,C2}$	3.4	8.4	0.5	3.0	3.2	8.1	3.6	3.8 3.7
$^2J_{C4,H3b}$	–3.7	–3.5	–2.0	–4.4	0.1	–3.0	–4.5	–5.4
$^2J_{C4,H3a}$	–2.7	–1.6	–4.7	–2.6	–2.5	–2.2	–5.4	–4.4 –4.1
MAD 29	2.29	3.41	2.53	2.20	2.24	3.19		
MAD 28	**0.83**	3.51	3.68	3.37	2.38	4.07		

to predict $^{2,3}J_{C,H}$ values of nitrogenated acyclic systems, taking into account all factors affecting the heteronuclear coupling constants.

4. Selection of Stereostructures Prior to Their Total Synthesis

4.1. 14 Years vs. 14 Days: A DFT–NMR Integrated Approach as a Guide for the Total Synthesis of Chiral Molecules

In the above-reported examples the QM calculation of NMR parameters was employed to assign the configuration of natural products, and here we report a recent application of the DFT–NMR integrated approach to support the total synthesis. In this case, it will be shown that an appropriate quantum chemical approach is a fast and convenient method to be applied prior to proceeding with the total synthesis of complex natural compounds. In detail, we report the analysis of the configuration of two natural compounds (kedarcidin chromophore and palu'amine)[68] and how the use of the quantum chemical approach could avoid loss of time and loss of resources employed in the total synthesis of wrong diastereoisomers. The structure of the kedarcidin chromophore has been revised over the last 14 years: the structure was first proposed by Leet and co-workers in 1992 (**30**, Scheme 22),[69] later revised to a β-amino ester[70] by Hirama et al. in 1997 (**31**, Scheme 22), and revised again through a total synthesis outlined by Myers et al. in 2007 (**32**, Scheme 22).[71] In particular, Myers[71] et al. synthesized the structure proposed by Hirama (i.e., **31**) and found several inconsistencies: (a) $^3J_{H10,H11} \approx 0$ vs. 5.4 Hz in CDCl₃ for the authentic kedarcidin chromophore; (b) the lack of an NOE between the pyridyl H-4′ and H-10, and the presence of an NOE between H-10 and H-12b; (c) mixture of atropisomers in both [D₆]DMSO and in C₆D₆, – one with the chlorine atom pointing toward the central core and the other one resulting from a 180° rotation of the pyridyl ring and with the chlorine atom pointing in the opposite direction with respect to the enediyne moiety. On the other hand, in accordance with the single atropisomer spectrum displayed by the natural product,[71] they argued that structure **32** derived by epimerization of the mycarose-bearing C-10 could not exist in the atropisomeric form in which the chlorine atom is oriented toward C-10. In conclusion, the efforts of Myers et al. in the synthesis of the wrong stereoisomers eventually allowed the correct structure to be established, but such efforts required a great amount of money and human resources. In order to suggest a straightforward method to be used prior to the total synthesis of molecules with complicated structures, we examined the structure and chemical shifts of the kedarcidine chromophore at the quantum chemical level by taking into account the wrong and the revised structures. First of all, we performed a conformational search, QM optimization of the energies and the geometries in vacuo, and single-point calculations by using a polar continuum model (PCM) for the simulation of the DMSO solvent, at the DFT level by using the MPW1PW91 functional with the 6-31G(d,p) basis set[9b] for the lowest-energy atropisomers for the two possible diastereomers (**31a** and **31b**, **32a** and **32b**; Figure 9) Interestingly, the result of our calculations was in
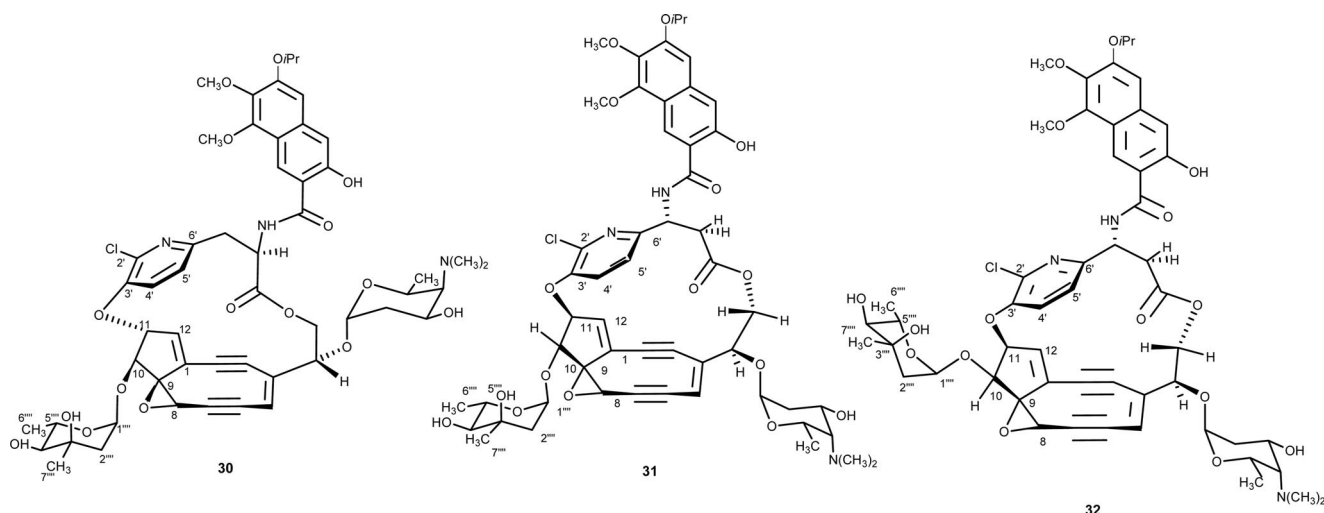
Scheme 22. Structure of kedarcidin chromophore as α-amino acid derivative **30** proposed by Leet in 1992, as β-amino ester **31** proposed by Hirama in 1997, and revised structure **32** proposed by Myers in 2007.

accordance with that proposed by Myers et al.:[71] (a) **31** exists in the atropisomeric form (the predicted differences of 1.8 and 1.3 kJ mol^{-1} accounting for a 1.8:1 and 1.3:1 ratio in vacuo and DMSO, respectively, versus the reported 2:1 ratio in [D$_6$]DMSO), and the atropisomer that presents the chlorine atom directed away from central core **31a** is the lowest in energy; (b) the calculated differences of 5.4 and 2.5 kJ mol^{-1} in vacuo and DMSO, respectively, for **32** confirms the presence of a single atropisomer, and as expected, atropisomer **32a** with the chlorine atom away from C-10 was predicted to be the lowest in energy. Moreover, we examined the results of the DFT calculation of the kedarcidin core fragment *J* values between H-10 and H-11 for **31a**, **31b**, **32a**, and **32b** by using the MPW1PW91 functional and the 6-311++G(2df,2p) basis set.[9b] In accordance with the experimental data collected by Myers et al., such values are predicted to be 0.1 Hz for **31a** and 0.1 Hz for **31b**. The values predicted for **32a** and **32b** are 6.1 and 4.7 Hz, respectively, and in comparison to the experimental value of 5.4 Hz reported in CDCl$_3$, they strongly support that the kedarcidin chromophore structure must be revised as **32**. Such results are in good agreement with that observed by Myers et al.,[71] suggesting that the kedarcidin chromophore could have in its most stable conformation only one predominant atropisomer (i.e., **32a**) characterized by the chlorine atom of the pyridyl ring oriented away from the core portion of the molecule (Figure 9).

To further validate the efficiency of our approach, we also examined the marine natural product palau'amine. In this case, the problem is associated with a hexacyclic structure containing eight stereogenic centers, whose relative configurations have not yet been confirmed by total synthesis. The initial structure proposed by Kinnel et al. (**33a**, Scheme 23)[72] had the relative configuration assigned as 6*R*,10*S*,11*R*,12*S*,16*S*,17*S*,18*R*,20*R*, and this results in a *cis* fusion between the D and E rings and the chlorine atom on the α-face of the molecule. Very recently, the isolation and structural elucidation of two additional palau'amine conge-
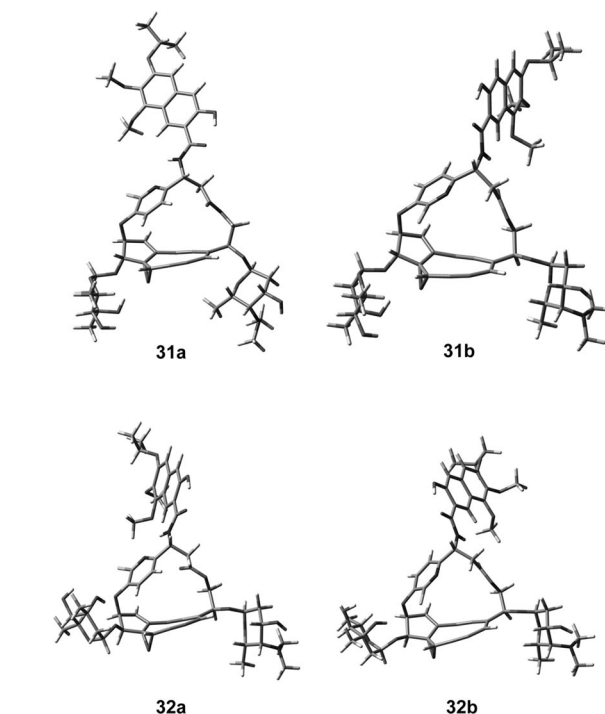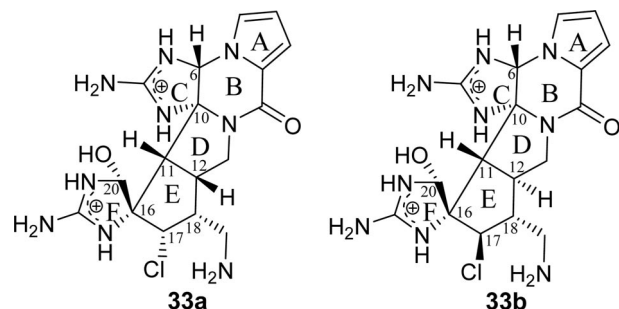

Figure 9. 3D models of possible kedarcidin chromophore atropisomers for **31** and **32**.

ners[73–75] prompted revision of the initial assignment of the relative configuration of palau'amine by NMR, computational methods,[73,76,77] correlation with related compounds,[74,75,78] and reisolation and characterization of palau'amine itself.[79] Proposed revised structure **33b** (Scheme 23) has the relative configuration assigned as 6*R*,10*S*,11*R*,12*R*,16*S*,17*R*,18*R*,20*R* and so a *trans* junction between the D and E rings and the chlorine atom on the β-face of the molecule. Due to the complexity of the problem, we tried to apply the quantum chemical approach for palau'amine. In particular, a conformational search was per-

formed on possible diastereoisomers **33a** and **33b** (Scheme 23), followed by full geometry and energy optimization at the quantum chemical level. At the DFT level and on the obtained geometries we calculated (Table 11) the diagnostic $^3J_{H,H}$ coupling constants for the D and E rings. As shown in Table 11, the calculated $^3J_{H,H}$ values are consistent with a *trans* junction between the D and E rings, and the suggested configuration at C-17 is *R*; particularly diagnostic is the calculated value of 13.2 Hz for $^3J_{H11,H12}$ in compound **33b**. The complete analysis of all the calculated *J* coupling constants of possible diastereoisomers **33a** and **33b**, outlined by the MAE (mean absolute error) parameter (Table 11), demonstrates a better fitting of model **33b** with the experimental NMR spectroscopic data reported in the literature,[73–78] and so with the proposed revised structure. Moreover, in this second example we also performed single-point GIAO calculations by using the MPW1PW91 functional and the 6-31G(d,p) basis set.[9b] Analysis of the model compounds was carried out by taking into consideration the calculated ^{13}C NMR values in DMSO (Table 12). In particular and concerning the ^{13}C NMR calculated results, we considered the $\Delta\delta$ (differences for experimental vs. calculated ^{13}C NMR chemical shifts) and MAE parameters. Through evaluation of the MAE values for models **33a** and **33b** (4.3 vs. 2.5, respectively), the GIAO calculated ^{13}C NMR chemical shifts indicated that compound **33b** fits better with the experimental data, confirming the revised structure of palau'amine recently proposed with a *trans* junction between the D and E rings and the chlorine atom on the β-face of the molecule (Figure 10).

Table 12. Comparison between experimental ^{13}C NMR chemical shifts in DMSO[79] with calculated ^{13}C NMR chemical shifts in DMSO [ppm] of diastereoisomers **33a** and **33b** and their $|\Delta\delta|$[a] values.

		33a		33b	
	$\delta_{exp.}$	$\delta_{calcd.}$	$|\Delta\delta|$[a]	$\delta_{calcd.}$	$|\Delta\delta|$[a]
C-6	67.5	73.0	5.5	67.1	0.4
C-10	79.4	84.7	5.3	84.0	4.6
C-11	55.3	54.8	0.5	54.7	0.6
C-12	40.6	42.9	2.3	39.1	1.5
C-13	44.8	51.0	6.2	46.2	1.4
C-16	70.3	77.5	7.2	73.1	2.8
C-17	73.7	69.9	3.8	76.4	2.7
C-18	47.0	41.1	5.9	51.5	4.5
C-19	40.2	43.5	3.3	44.7	4.5
C-20	82.2	85.6	3.4	83.7	1.5
MAE[b]		4.3		2.5	

[a] $|\Delta\delta| = |\delta_{exp.} - \delta_{calcd.}|$, absolute difference of the experimental and calculated ^{13}C NMR chemical shifts. [b] Mean average error = $\Sigma[|\delta_{exp.} - \delta_{calcd.}|]/n$.
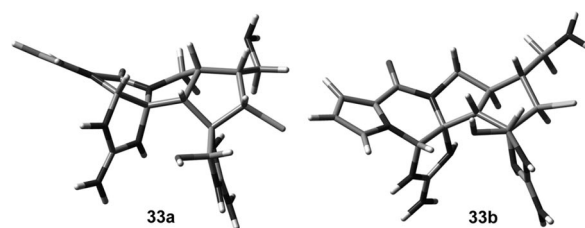

Figure 10. 3D models of diastereoisomers **33a** and **33b** of palau'amine.

4.2. Prediction of the Stereostructure of Elatenyne

The work reported by Goodman[80] et al. in 2008 regarded the assignment of the relative configuration of the marine natural product elatenyne. The original structure of elatenyne[81] (**34**) was, thanks to following synthetic studies, reproposed as 2,2′-bifuranyl system[82] **35** (Scheme 24). After a brief validation of our DFT–NMR method[8] for its application to the stereochemical investigation of the bifuranyl system, they used this technique to predict the stereostructure of elatenyne. NMR chemical shifts were calculated for all 32 possible diastereoisomers of **35** as well as for pyranopyran structure **34** originally proposed. As previously suggested,[8] the experimental data was compared by two methods: (1) the linear correlation coefficients *r* between all pairs of calculated and experimental chemical shifts and (2) the sum, or the average, of the absolute differences between the empirically scaled calculated chemical shifts and the experimental chemical shifts ($\Delta\delta$). Besides the two above-described analysis methods, the authors applied the approach of Rzepa[83] for carbon substituted with heavy atoms (C2, C7, and C12), or tried to exclude these carbon atoms from all analyses, and they obtained consistent results in all cases. In particular, the most likely candidate for the structure of elatenyne is **35v**, although **35e′**, **35z**, and **35s** remain plausible. Pyranopyran structure **34** gives a particularly poor match in terms of both correlation coefficient and mean $|\Delta\delta|$. The Goodman work represents the begin-

Scheme 23. Original **33a** and revised **33b** structure of palau'amine.

Table 11. Comparison between experimental (DMSO)[79] and calculated (in vacuo) $^3J_{H,H}$ values [Hz] for the D and E rings of stereoisomers **33a** and **33b**.

	Calcd.		Exp.
	33a	33b	
$^3J_{H11,H12}$	8.8	13.2	14.4
$^3J_{H12,H18}$	9.0	9.6	9.0
$^3J_{H18,H17}$	10.3	9.6	9.0
$^3J_{H12,H13\alpha}$	8.5	9.0	10.2
$^3J_{H12,H13\beta}$	9.9	7.0	7.2
MAE[a]	2.3	0.7	

[a] Mean average error = $\Sigma[|J_{exp.} - J_{calcd.}|]/n$.

ning of the elatenyne confirmation structure process, suggesting only four possible candidates (Scheme 25) for the following synthetic studies.
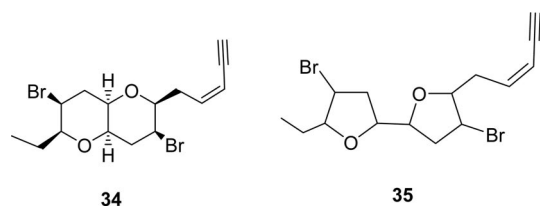
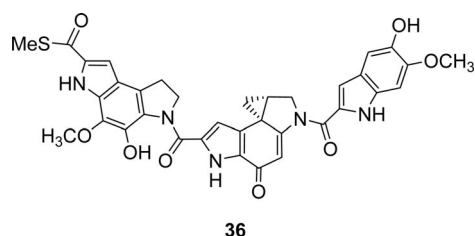Scheme 24. Original and revised structure of elatenyne.
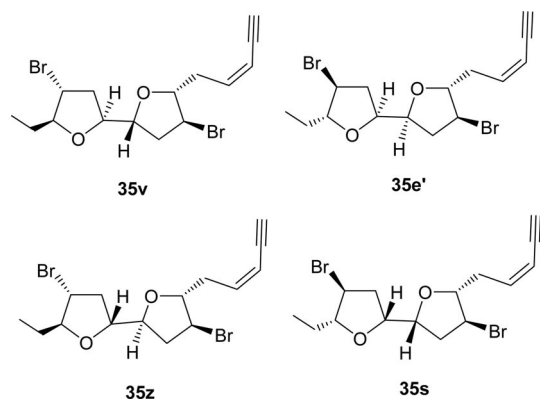
Scheme 25. Molecular structure of the most likely candidates for the stereostructure of elatenyne.

5. Quantum Mechanical Calculation of NMR Parameters as a Tool for the Characterization of Ligand–DNA Interactions

(+)-Yatakemycin[84–88] (**36**, Scheme 26), isolated from the culture broth of *Streptomyces* sp. TP-A0356,[89] represents the newest and most potent member of a class of natural antitumor compounds.[84–88] Its biological activity is derived from the ability of alkylating specific adenine residues in the minor groove of AT-rich tracts. In particular, the alkylation reaction proceeds by nucleophilic attack by adenine N3 on the reactive cyclopropyl ring of the ligand, upon binding to the DNA. The covalent complex d(GAC-TAATTGAC)-(GTCAATTAGTC)–(+)-yatakemycin has been analyzed by an approach based on NMR spectroscopic data integrated by quantum mechanical calculations of the ^{1}H NMR chemical shifts to get key structural features for the development of more powerful and more selective anticancer drugs.[24] The study of this macromolecular system shows that the calculation of NMR parameters is not limited to structure elucidation of molecules with a limited number of atoms, but it may also be extended to larger systems to achieve essential information about ligand–macromolecule interactions.[24] In particular, stereostructural studies of bioactive compounds of natural origin could be also carried out on the ligand conformation within the binding site of the biological target. Moreover, the QM-based approach can be useful in cases where dipolar cou-

plings between ligand and macromolecule are uncertain or unavailable; it can also provide useful and additional data to standard spectroscopic tools applied in the characterization of drug–DNA/protein complexes. Firstly, by a well-established NMR strategy,[90] the ^{1}H NMR chemical shifts of the DNA duplex covalently bound to the ligand were assigned, and the binding site was mapped out by monitoring the experimental ^{1}H NMR resonance shifts between the free and bound state of DNA.[24] The NMR receptor-based approach did not allow the adenine involved in the covalent bond to **36** to be distinguished, because candidate residues A5 and A6 showed comparable chemical shift perturbations between the free and bound state of DNA. In order to determine which adenine was responsible for nucleophilic attack on the cyclopropane ring of the ligand, a new faster and easier method was devised as an alternative to the full collection of experimental restraints necessary to obtain the 3D experimental structure of the covalent complex. In particular, an approach based on integrated NMR experimental data with GIAO ^{1}H NMR DFT calculated values was proposed to study ligand–macromolecule interactions, going well over the successful application of ^{1}H and ^{13}C NMR chemical shift calculations in the structure elucidation of organic molecules,[8a,9b,28] in the interpretation of polymer spectra[28d] and in the conformational analysis of peptides,[91–93] oligosaccharides,[94] and calixarenes.[95] Thus, two 3D models were built where **36** was covalently bound to A5 or A6 (model A or B, respectively; Figure 11a,b), and starting from the NMR structure of duocarmycin SA covalently linked to the DNA duplex (PDB[96] archive code 1DSA)[97] **36** was built and docked in the minor groove.[24] In order to perform quantum mechanical calculations in a reasonable computation time and with a reliable model, only six base pairs of the DNA were considered (Figure 11). For these reduced models, ^{1}H NMR chemical shifts were calculated at the DFT/MPW1PW91 theoretical level with the 6-31g(d,p) basis set, as such a combination has provided satisfactory results with reasonable computational effort for the calculation of NMR parameters of medium–large organic molecules.[3,28b,98] Besides the A5 and A6 resonances, the imino proton of T17 and H-3′ of T18 showed a dramatic variation upon binding of yatakemicin, –2.08 and 1.5 ppm, respectively (Figure 12), and for this reason their values were considered diagnostic and compared with the experimental data. The analysis of the data put in evidence that only one of the two structural hypotheses presented a satisfactory agreement with the experimental data set. A good accordance, in fact, is observed between the calculated ^{1}H NMR chemical shifts of model A (alkylation at A5) and the experimental data, along with the MAE and the correlation coefficients (Table 13). Residual discrepancies between experimental and theoretical ^{1}H NMR chemical shifts for model A could probably be due to the absence of solvent in the calculations or to the low level of theory that was chosen according to the complexity of the system. On the other hand, model B (alkylation at A6) presented large differences between the calculated and experimental ^{1}H NMR resonances on almost all protons considered

(Table 13), allowing this hypothesis to be discarded and suggesting nucleophilic attack by N3 of adenine 5. Further corroboration was provided by analysis of key NOE contacts between the DNA duplex and (+)-yatakemycin, confirming the reliability of the presented methodology.[24] In particular, the H-28 resonance of the ligand ($\delta = 3.83$ ppm) shows dipolar effects with H-1′ ($\delta = 5.03$ ppm) of the A5 residue and H-8 ($\delta = 8.15$ ppm) of the A6 residue. The distances of H-28 from H-1′ and H-8 are, respectively, 1.96 and 3.46 Å (Figure 13), whereas in model B they are expected at 6.15 and 5.02 Å. Thus, model A better reproduces the experimental values, which validates the results obtained independently through the presented quantum chem-

Table 13. Significant ^{1}H NMR calculated [MPW1PW91/6-31G(d,p) level] chemical shifts [ppm] for models A and B, and the corresponding ^{1}H NMR experimental data of DNA bound to 36. The term $\Delta(\delta_{calcd.} - \delta_{exp.})$ is the difference between calculated and experimental chemical shifts.

RES.	H	$\delta(^1H)_{calcd.}$		$\delta_{exp.}$	$\Delta(\delta_{calcd.} - \delta_{exp.})$	
		A	B		A	B
A5	8	8.68	8.06	8.49	0.19	–0.43
	2′	2.63	2.29	2.59	0.04	–0.30
	2′′	2.43	1.93	2.89	–0.46	–0.95
	1′	5.70	5.78	5.03	0.67	0.74
A6	8	8.26	9.03	8.15	0.10	0.87
	2′	1.89	1.79	2.33	–0.44	–0.55
	2′′	2.83	2.66	2.44	0.39	0.22
	1′	5.87	6.10	5.32	0.55	0.78
T17	N3H	11.43	10.80	11.50	–0.07	–0.70
T18	3′	4.68	4.79	4.50	0.18	0.28
MAE[a]		0.31	0.58			
R[b]		0.9932	0.978			

[a] Mean absolute error (MAE) found for ^{1}H NMR chemical shifts of models A and B vs. [1]H experimental values: MAE = $\sum[|\delta_{exp.} - \delta_{calcd.}|]/n$. [b] Correlation coefficient obtained by linear fitting of calculated ($\delta_{calcd.}$) vs. experimental ($\delta_{exp.}$) ^{1}H NMR chemical shifts.

Scheme 26. Molecular structures of (+)-yatakemycin (36).

a) **b)**
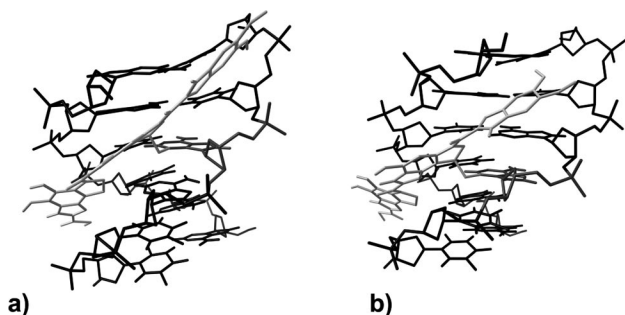
Figure 11. 3D models of (+)-yatakemycin (36) covalently bound to A5 (a) and to A6 (b). For the nucleic acid the two models contain only the base-pairs C3:G20 to T8:A15. The DNA and ligand are represented in tube. The DNA chains are depicted in black except the adenine (in dark grey) covalently bound to ligand and 36 is colored in light grey. The figure highlights the covalent bond with adenine N3 and how the ligand assumes a curved conformation in the minor groove.
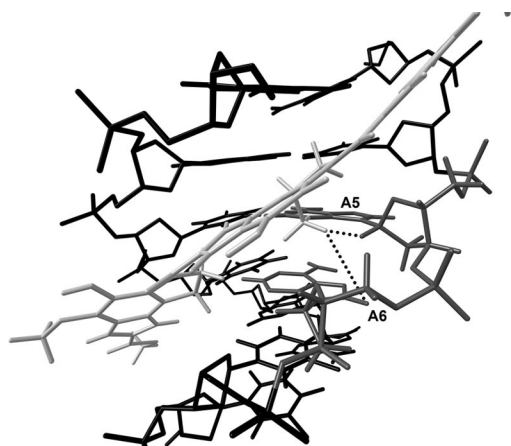

Figure 13. 3D model (duplex DNA base-pair region C3:G20 to T8:A15) of (+)-yatakemycin (36) covalently bound to A5. The black broken lines show the NOE contacts experimentally observed and well reproduced by model A.

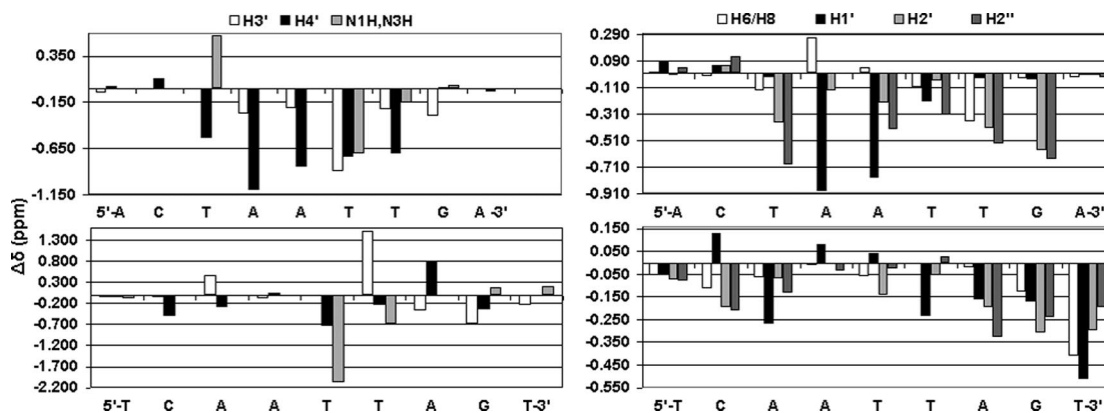Figure 12. Chemical shift differences ($\Delta\delta = \delta_{bound\ DNA} - \delta_{free\ DNA}$) plots for the sugar and base protons of the DNA duplex. The base-pairs G1–C22 and C11–G12 are not considered because they do not show resonance shifts.

ical methodology.[24] It is noteworthy that, due to the size of the system analyzed, the tradeoff between computation time and reliability of calculated values to reproduce experimental data justifies the use of a limited theoretical model, but the application of higher levels of theory is encouraged.

6. Conclusions

In the present contribution, diverse case studies are reported that use calculations of chemical shifts and *J* coupling constants at the QM theoretical level for conformational and configurational analysis of natural products. In particular, the described cases highlight how QM calculated NMR properties can be tailored and combined depending on the organic compound under examination.

Besides the use of QM calculation of NMR parameters in the structural studies, the fast and convenient quantum chemical approach could be applied to lead the total synthesis of complex natural compounds towards the correct diastereoisomers, saving time and employed resources.

Recently, the authors analyzed the covalent complex formed between d(GACTAATTGAC)-(GTCAATTAGTC) and (+)-yatakemycin by an approach based on NMR spectroscopic data integrated by quantum mechanical calculations of ^{1}H NMR chemical shifts. This new approach involving the QM calculation of NMR parameters could represent a faster and easier strategy for the study of drug–macromolecule interactions and could be considered an alternative or a complementary tool of the most commonly employed spectroscopic techniques.

[1] J. M. Seco, E. Quiñoà, R. Riguera, *Chem. Rev.* **2004**, *104*, 17–117.

[2] K. C. Nicolaou, S. A. Snyder, *Angew. Chem. Int. Ed.* **2005**, *44*, 1012–1044.

[3] G. Bifulco, P. Dambruoso, L. Gomez-Paloma, R. Riccio, *Chem. Rev.* **2007**, *107*, 3744–3779.

[4] M. Karplus, *J. Chem. Phys.* **1959**, *30*, 11–15.

[5] a) A. W. Overhauser, *Phys. Rev.* **1953**, *92*, 411–415; b) D. Neuhaus, M. P. Williamson, *The Nuclear Overhauser Effect in Structural and Conformational Analysis*, 2nd ed., Wiley-VCH, New York, **2000**.

[6] N. Matsumori, D. Kaneno, M. Murata, H. Nakamura, K. Tachibana, *J. Org. Chem.* **1999**, *64*, 866–876.

[7] a) Y. Kobayashi, J. Lee, K. Tezuka, Y. Kishi, *Org. Lett.* **1999**, *1*, 2177–2180; b) J. Lee, Y. Kobayashi, K. Tezuka, Y. Kishi, *Org. Lett.* **1999**, *1*, 2181–2184.

[8] a) G. Barone, L. Gomez-Paloma, D. Duca, A. Silvestri, R. Riccio, G. Bifulco, *Chem. Eur. J.* **2002**, *8*, 3233–3239; b) G. Barone, D. Duca, A. Silvestri, L. Gomez-Paloma, R. Riccio, G. Bifulco, *Chem. Eur. J.* **2002**, *8*, 3240–3245.

[9] a) J. R. Cheeseman, G. W. Trucks, T. A. Keith, M. J. Frisch, *J. Chem. Phys.* **1996**, *104*, 5497–5509; b) P. Cimino, L. Gomez-Paloma, D. Duca, R. Riccio, G. Bifulco, *Magn. Reson. Chem.* **2004**, *42*, 26–33.

[10] a) M. Elyashberg, K. Blinov, A. Williams, *Magn. Reson. Chem.* **2009**, *47*, 371–389; b) M. E. Elyashberg, K. A. Blinov, A. J. Williams, *Magn. Reson. Chem.* **2009**, *47*, 333–341; c) M. Elyashberg, K. Blinov, S. Molodtsov, Y. Smurnyy, A. J. Williams, T. Churanova, *J. Cheminf.* **2009**, 1:3.

[11] a) M. E. Elyashberg, A. J. Williams, G. E. Martin, *Prog. NMR Spectrosc.* **2008**, *53*, 1–104; b) K. A. Blinov, Y. D. Smurnyy, T. S. Churanova, M. E. Elyashberg, A. J. Williams, *Chemom.*

Intell. Lab. Syst. **2009**, *97*, 91–97; c) K. A. Blinov, Y. D. Smurnyy, M. E. Elyashberg, T. S. Churanova, M. Kvasha, C. Steinbeck, B. A. Lefebvre, A. J. Williams, *J. Chem. Inf. Model.* **2008**, *48*, 550–555; d) Y. D. Smurnyy, K. A. Blinov, T. S. Churanova, M. E. Elyashberg, A. J. Williams, *J. Chem. Inf. Model.* **2008**, *48*, 128–134.

[12] a) R. J. Ditchfield, *Chem. Phys.* **1972**, *56*, 5688–5691; b) K. Wolinski, J. F. Hinton, P. Pulay, *J. Am. Chem. Soc.* **1990**, *112*, 8251–8260.

[13] a) W. F. van Gunsteren, H. J. C. Berendsen, *Angew. Chem. Int. Ed. Engl.* **1990**, *29*, 992–1023; b) H. D. Höltje, W. Sippl, G. Folkers, *Molecular Modeling Basic Principles and Applications* (Eds.: R. Mannhold, H. Kubinyi, H. Timmerman), Wiley-VCH, Weinheim, **2003**, vol. 5, pp. 23–36.

[14] G. Chang, W. C. Guida, W. C. Still, *J. Am. Chem. Soc.* **1989**, *111*, 4379–4386.

[15] M. J. S. Dewar, E. G. Zoebisch, E. F. Healy, J. J. P. Stewart, *J. Am. Chem. Soc.* **1985**, *107*, 3902–3909.

[16] J. J. P. Stewart, *J. Comput. Chem.* **1989**, *10*, 209–220.

[17] a) P. Hohenberg, W. Kohn, *Phys. Rev. B* **1964**, *136*, 864–871; b) W. Kohn, L. J. Sham, *Phys. Rev. A* **1965**, *140*, 1133–1138.

[18] G. Bifulco, C. Bassarello, R. Riccio, L. Gomez-Paloma, *Org. Lett.* **2004**, *6*, 1025–1028.

[19] A. Bagno, F. Rastrelli, G. Saielli, *Chem. Eur. J.* **2006**, *12*, 5514–5525.

[20] S. D. Rychnovsky, *Org. Lett.* **2006**, *8*, 2895–2898.

[21] J. Yang, S.-X. Huang, Q.-S. Zhao, *J. Phys. Chem. A* **2008**, *112*, 12132–12139.

[22] R. Barthwal, P. Agrawal, A. N. Tripathi, U. Sharma, N. R. Jagannathan, G. Govil, *Arch. Biochem. Biophys.* **2008**, *474*, 48–64.

[23] F. Pichierri, V. Galasso, *J. Phys. Chem. A* **2007**, *111*, 5898–5906.

[24] S. Di Micco, D. L. Boger, R. Riccio, G. Bifulco, *Eur. J. Org. Chem.* **2008**, 2454–2462.

[25] S. Rosselli, M. Bruno, A. Maggio, G. Bellone, C. Formisano, C. A. Mattia, S. Di Micco, G. Bifulco, *Eur. J. Org. Chem.* **2007**, 2504–2510.

[26] J. A. Dale, H. S. Mosher, *J. Am. Chem. Soc.* **1973**, *95*, 512–519.

[27] M. J. Frisch, G. W. Trucks, H. B. Schlegel, G. E. Scuseria, M. A. Robb, J. R. Cheeseman, J. A. Montgomery Jr., T. Vreven, K. N. Kudin, J. C. Burant, J. M. Millam, S. S. Iyengar, J. Tomasi, V. Barone, B. Mennucci, M. Cossi, G. Scalmani, N. Rega, G. A. Petersson, H. Nakatsuji, M. Hada, M. Ehara, K. Toyota, R. Fukuda, J. Hasegawa, M. Ishida, T. Nakajima, Y. Honda, O. Kitao, H. Nakai, M. Klene, X. Li, J. E. Knox, H. P. Hratchian, J. B. Cross, V. Bakken, C. Adamo, J. Jaramillo, R. Gomperts, R. E. Stratmann, O. Yazyev, A. J. Austin, R. Cammi, C. Pomelli, J. W. Ochterski, P. Y. Ayala, K. Morokuma, G. A. Voth, P. Salvador, J. J. Dannenberg, V. G. Zakrzewski, S. Dapprich, A. D. Daniels, M. C. Strain, O. Farkas, D. K. Malick, A. D. Rabuck, K. Raghavachari, J. B. Foresman, J. V. Ortiz, Q. Cui, A. G. Baboul, S. Clifford, J. Cioslowski, B. B. Stefanov, G. Liu, A. Liashenko, P. Piskorz, I. Komaromi, R. L. Martin, D. J. Fox, T. Keith, M. A. Al-Laham, C. Y. Peng, A. Nanayakkara, M. Challacombe, P. M. W. Gill, B. Johnson, W. Chen, M. W. Wong, C. Gonzalez, J. A. Pople, *Gaussian 03*, Revision B.05, Gaussian, Inc., Wallingford, CT, **2004**.

[28] a) M. Stahl, U. J. Schopfer, *J. Chem. Soc. Perkin Trans. 2* **1997**, 905–908; b) D. Duca, G. Bifulco, G. Barone, A. Casapullo, A. Fontana, *J. Chem. Inf. Comput. Sci.* **2004**, *44*, 1024–1030; c) J. W. Bausch, R. C. Rizzo, L. G. Sneddon, A. E. Wille, R. E. Williams, *Inorg. Chem.* **1996**, *35*, 131–135; d) A. C. de Dios, *Prog. NMR Spectrosc.* **1996**, *29*, 229–278.

[29] C. Bassarello, G. Bifulco, P. Montoro, A. Skhirtladze, E. Kemertelidze, C. Pizza, S. Piacente, *Tetrahedron* **2007**, *63*, 148–154.

[30] C. Bassarello, G. Bifulco, P. Montoro, A. Skhirtladze, M. Benidze, E. Kemertelidze, C. Pizza, S. Piacente, *J. Agric. Food Chem.* **2007**, *55*, 6636–6642.

[31] a) C. Adamo, V. Barone, *J. Chem. Phys.* **1998**, *108*, 664–675; b) C. Adamo, V. Barone, *J. Chem. Phys.* **1999**, *110*, 6158–6170.

[32] B. Vera, A. D. Rodríguez, E. Avilés, Y. Ishikawa, *Eur. J. Org. Chem.* **2009**, 5327–5336.

[33] E. Fattorusso, P. Luciano, A. Romano, O. Taglialatela-Scafati, G. Appendino, M. Borriello, C. Fattorusso, *J. Nat. Prod.* **2008**, *71*, 1988–1992.

[34] I. Ohtani, T. Kusumi, Y. Kashman, H. Kakisawa, *J. Am. Chem. Soc.* **1991**, *113*, 4092–4096.

[35] K. C. Nicolaou, M. O. Frederick, *Angew. Chem. Int. Ed.* **2007**, *46*, 5278–5282.

[36] A. R. Gallimore, J. B. Spencer, *Angew. Chem. Int. Ed.* **2006**, *45*, 4406–4413.

[37] a) M. Murata, T. Iwashita, A. Yokoyama, M. Sasaki, T. Yasumoto, *J. Am. Chem. Soc.* **1992**, *114*, 6594–6596; b) M. Murata, H. Naoki, T. Iwashita, S. Matsunaga, M. Sasaki, A. Yokoyama, T. Yasumoto, *J. Am. Chem. Soc.* **1993**, *115*, 2060–2062; c) M. Murata, H. Naoki, S. Matsunaga, M. Satake, T. Yasumoto, *J. Am. Chem. Soc.* **1994**, *116*, 7098–7107; d) M. Satake, S. Ishida, T. Yasumoto, *J. Am. Chem. Soc.* **1995**, *117*, 7019–7020.

[38] a) M. Sasaki, T. Nonomura, M. Murata, K. Tachibana, *Tetrahedron Lett.* **1995**, *36*, 9007–9010; b) M. Sasaki, T. Nomomura, M. Murata, K. Tachibana, T. Yasumoto, *Tetrahedron Lett.* **1995**, *36*, 9011–9014; c) M. Sasaki, T. Nonomura, M. Murata, K. Tachibana, *Tetrahedron Lett.* **1994**, *35*, 5023–5026; d) M. Sasaki, N. Matsumori, T. Muruyama, T. Nonomura, M. Murata, K. Tachibana, *Angew. Chem. Int. Ed. Engl.* **1996**, *35*, 1672–1675; e) T. Nonomura, M. Sasaki, N. Matsumori, M. Murata, K. Tachibana, T. Yasumoto, *Angew. Chem. Int. Ed. Engl.* **1996**, *35*, 1675–1678.

[39] a) W. Zheng, J. A. De Mattei, J.-P. Wu, J. J.-W. Duan, L. R. Cook, H. Oinuma, Y. Kishi, *J. Am. Chem. Soc.* **1996**, *118*, 7946–7968; b) L. R. Cook, H. Oinuma, M. A. Semones, Y. Kishi, *J. Am. Chem. Soc.* **1997**, *119*, 7928–7937.

[40] The structure of brevetoxin B was determined by spectroscopy and X-ray analysis, and it was confirmed by chemical synthesis: a) Y.-Y. Lin, M. Risk, S. M. Ray, D. Van Engen, J. Clardy, J. Golik, J. C. James, K. Nakanishi, *J. Am. Chem. Soc.* **1981**, *103*, 6773–6775; b) M. S. Lee, D. J. Repeta, K. Nakanishi, M. G. Zagorksi, *J. Am. Chem. Soc.* **1986**, *108*, 7855–7856; c) K. C. Nicolaou, E. A. Theodorakis, F. P. J. T. Rutjes, J. Tiebes, M. Sato, E. Untersteller, X.-Y. Xiao, *J. Am. Chem. Soc.* **1995**, *117*, 1171–1172; d) K. C. Nicolaou, F. P. J. T. Rutjes, E. Theodorakis, J. Tiebes, M. Sato, E. Unterstellar, *J. Am. Chem. Soc.* **1995**, *117*, 1173–1174; e) K. C. Nicolaou, E. A. Theodorakis, F. P. J. T. Rutjes, M. Sato, J. Tiebes, X.-Y. Xiao, C.-K. Hwang, M. E. Duggan, Z. Yang, E. A. Couladouros, F. Sato, J. Shin, H.-M. He, T. Bleckman, *J. Am. Chem. Soc.* **1995**, *117*, 1023–10251; f) K. C. Nicolaou, F. P. J. T. Rutjes, E. A. Theodorakis, J. Tiebes, M. Sato, E. Unterstellar, *J. Am. Chem. Soc.* **1995**, *117*, 10252–10263; g) K. C. Nicolaou, *Angew. Chem. Int. Ed. Engl.* **1996**, *35*, 588–607.

[41] M. A. Muñoz, P. Joseph-Nathan, *Magn. Reson. Chem.* **2009**, *47*, 578–584.

[42] M. A. Muñoz, O. Muñoz, P. Joseph-Nathan, *J. Nat. Prod.* **2006**, *69*, 1335–1340.

[43] K. W. Wiitala, C. J. Cramer, T. R. Hoye, *Magn. Reson. Chem.* **2007**, *45*, 819–829.

[44] a) I. Alkorta, J. Elguero, *New J. Chem.* **1998**, *22*, 381–385; b) J. A. Gomes, R. B. Mallion, *Chem. Rev.* **2001**, *101*, 1349–1384; c) C. S. Wannere, P. Schleyer, *Org. Lett.* **2003**, *5*, 605–608.

[45] J. Boyd, N. R. Skrynnikov, *J. Am. Chem. Soc.* **2002**, *124*, 1832–1833.

[46] J. X. Pu, S. X. Huang, J. Ren, W. L. Xiao, L. M. Li, R. T. Li, L. B. Li, T. G. Liao, L. G. Lou, H. J. Zhu, H. D. Sun, *J. Nat. Prod.* **2007**, *70*, 1707–1711.

[47] S. G. Smith, J. M. Goodman, *J. Org. Chem.* **2009**, *74*, 4597–4607.

[48] A. M. Belostotskii, *J. Org. Chem.* **2008**, *73*, 5723–5731.

[49] J. J. Poza, C. Jiménez, J. Rodríguez, *Eur. J. Org. Chem.* **2008**, 3960–3969.

[50] C. Bassarello, A. Zampella, M. C. Monti, L. Gomez-Paloma, M. V. D'Auria, R. Riccio, G. Bifulco, *Eur. J. Org. Chem.* **2006**, 604–609.

[51] R. Krishnamoorthy, L. D. Vazquez-Serrano, J. A. Turk, J. A. Kowalski, A. G. Benson, N. T. Breaux, M. A. Lipton, *J. Am. Chem. Soc.* **2006**, *128*, 15392–15393.

[52] A. Zampella, M. V. D'Auria, L. Gomez-Paloma, A. Casapullo, L. Minale, C. Debitus, Y. Henin, *J. Am. Chem. Soc.* **1996**, *118*, 6202–6209.

[53] M. V. D'Auria, A. Zampella, L. Gomez-Paloma, L. Minale, C. Debitus, C. Roussakis, V. Le Bert, *Tetrahedron* **1996**, *52*, 9589–9596.

[54] A. Zampella, A. Randazzo, N. Borbone, S. Luciani, L. Trevisi, C. Debitus, M. V. D'Auria, *Tetrahedron Lett.* **2002**, *43*, 6163–6166.

[55] J. C. Thoen, A. I. Morales-Ramos, M. A. Lipton, *Org. Lett.* **2002**, *4*, 4455–4458.

[56] N. Oku, K. R. Gustafson, L. K. Cartner, J. A. Wilson, N. Shigematsu, S. Hess, L. K. Pannell, M. R. Boyd, J. B. McMahon, *J. Nat. Prod.* **2004**, *67*, 1407–1411.

[57] M. T. Cancès, B. Mennucci, J. Tomasi, *J. Chem. Phys.* **1997**, *107*, 3032–3041.

[58] Calculations of *erythro* and *threo* forms of AGDHE$_{2,3}$ were performed by varying the C-4 center. Because the two sets of calculations pointed to the same results, and on the basis of the results of the calculation regarding AGDHE$_{3,4}$ we reported, for the sake of simplicity, only the results of the set of calculations containing the correct relative configuration of C-4. The same considerations apply for fragment AGDHE$_{3,4}$, this time by varying C-2. Also in this case, we reported only the set of calculations containing the correct configuration of C-2.

[59] A. Zampella, R. D'Orsi, V. Sepe, A. Casapullo, M. C. Monti, M. V. D'Auria, *Org. Lett.* **2005**, *7*, 3585–3588.

[60] A. Plaza, G. Bifulco, J. L. Keffer, J. R. Lloyd, H. L. Baker, C. A. Bewley, *J. Org. Chem.* **2009**, *74*, 504–512.

[61] E. Manzo, M. Gavagnin, G. Bifulco, P. Cimino, S. Di Micco, M. L. Ciavatta, Y. W. Guo, G. Cimino, *Tetrahedron* **2007**, *63*, 9970–9978.

[62] a) M. Hashimoto, T. Kan, K. Nozaki, M. Yanagiya, H. Shirahama, T. Matsumoto, *Tetrahedron Lett.* **1988**, *29*, 1143–1144; b) M. Hashimoto, T. Kan, K. Nozaki, M. Yanagiya, H. Shirahama, T. Matsumoto, *J. Org. Chem.* **1990**, *55*, 5088–5107.

[63] A. Bax, D. G. Davis, *J. Magn. Reson.* **1985**, *63*, 207–213.

[64] *MacroModel, version 8.5*, Schrödinger LLC, New York, **2003**.

[65] J. J. Poza, C. Jiménez, J. Rodríguez, *Eur. J. Org. Chem.* **2008**, 3960–3969.

[66] A. Ardá, C. Jiménez, J. Rodríguez, *Eur. J. Org. Chem.* **2006**, 3645–3651.

[67] a) C. Bassarello, G. Bifulco, A. Evidente, R. Riccio, L. Gomez-Paloma, *Tetrahedron Lett.* **2001**, *42*, 8611–8613; b) R. T. Williamson, I. P. Singh, W. H. Gerwick, *Tetrahedron* **2004**, *60*, 7025–7033; c) P. Dambruoso, C. Bassarello, G. Bifulco, G. Appendino, A. Battaglia, A. Guerrini, G. Fontana, L. Gomez-Paloma, *Tetrahedron Lett.* **2005**, *46*, 3411–3415; d) A. Arda, J. Rodríguez, R. Nieto, C. Bassarello, L. Gomez-Paloma, G. Bifulco, C. Jimenez, *Tetrahedron* **2005**, *61*, 10093–10098.

[68] M. G. Chini, R. Riccio, G. Bifulco, *Magn. Reson. Chem.* **2008**, *46*, 962–968.

[69] J. E. Leet, D. R. Schroeder, D. R. Langley, K. L. Colson, S. Huang, S. E. Klohr, M. S. Lee, J. Colik, S. J. Hofstead, T. W. Doyle, J. A. Matson, *J. Am. Chem. Soc.* **1993**, *115*, 8432–8443.

[70] S. Kawata, S. Ashizawa, M. Hirama, *J. Am. Chem. Soc.* **1997**, *119*, 12012–12013.

[71] F. Ren, P. C. Hogan, A. J. Anderson, A. G. Myers, *J. Am. Chem. Soc.* **2007**, *129*, 5381–5383.

[72] R. B. Kinnel, H. P. Gehrken, P. J. Scheuer, *J. Am. Chem. Soc.* **1993**, *115*, 3376–3377.

[73] A. Grube, M. Köck, *Angew. Chem. Int. Ed.* **2007**, *46*, 2320–2324.

[74] H. Kobayashi, K. Kitamura, K. Nagai, Y. Nakao, N. Fusetani, R. W. M. van Soest, S. Matsunaga, *Tetrahedron Lett.* **2007**, *48*, 2127–2129.

[75] M. S. Buchanan, A. R. Carroll, R. Addepalli, V. M. Avery, J. N. A. Hooper, R. J. Quinn, *J. Org. Chem.* **2007**, *72*, 2309–2317.

[76] M. Köck, A. Grube, I. B. Seiple, P. S. Baran, *Angew. Chem. Int. Ed.* **2007**, *46*, 6586–6594.

[77] T. A. Cernak, J. L. Gleason, *J. Org. Chem.* **2008**, *73*, 102–110.

[78] B. A. Lanman, L. E. Overman, R. Paulini, N. S. White, *J. Am. Chem. Soc.* **2007**, *129*, 12896–12900.

[79] M. S. Buchanan, A. R. Carroll, R. J. Quinn, *Tetrahedron Lett.* **2007**, *48*, 4573–4574.

[80] S. G. Smith, R. S. Paton, J. W. Burton, J. M. Goodman, *J. Org. Chem.* **2008**, *73*, 4053–4062.

[81] J. G. Hall, J. A. Reiss, *Aust. J. Chem.* **1986**, *39*, 1401–1409.

[82] H. M. Sheldrake, C. Jamieson, J. W. Burton, *Angew. Chem. Int. Ed.* **2006**, *45*, 7199–7202.

[83] D. C. Braddock, H. S. Rzepa, *J. Nat. Prod.* **2008**, *71*, 728–730.

[84] J. P. Parrish, D. B. Kastrinsky, S. E. Wolkenberg, Y. Igarashi, D. L. Boger, *J. Am. Chem. Soc.* **2003**, *125*, 10971–10976.

[85] M. S. Tichenor, D. B. Kastrinsky, D. L. Boger, *J. Am. Chem. Soc.* **2004**, *126*, 8396–8398.

[86] M. S. Tichenor, J. D. Trzupek, D. B. Kastrinsky, F. Shiga, I. Hwang, D. L. Boger, *J. Am. Chem. Soc.* **2006**, *128*, 15683–15696.

[87] D. L. Boger, D. L. Hertzog, B. Bollinger, D. S. Johnson, H. Cai, J. Goldberg, P. Turnbull, *J. Am. Chem. Soc.* **1997**, *119*, 4977–4986.

[88] K. Okano, H. Tokuyama, T. Fukuyama, *J. Am. Chem. Soc.* **2006**, *128*, 7136–7137.

[89] Y. Igarashi, K. Futamata, T. Fujita, A. Sekine, H. Senda, H. Naoki, T. Furumai, *J. Antibiot.* **2003**, *56*, 107–113.

[90] a) D. E. Wemmer, B. R. Reid, *Annu. Rev. Phys. Chem.* **1985**, *36*, 105–137; b) K. Wüthrich in *NMR of Proteins and Nucleic Acids*, Wiley, New York, **1986**, pp. 1–304; c) W. J. Chazin, K. Wüthrich, S. Hyberts, M. Rance, W. A. Denny, W. Leupin, *J. Mol. Biol.* **1986**, *190*, 439–453; d) D. J. Patel, L. Shapiro, D. Hare, *Quart. Rev. Biophys.* **1987**, *20*, 35–112; e) D. J. Patel, L. Shapiro, D. Hare, *Annu. Rev. Biophys. Biophys. Chem.* **1987**, *16*, 423–454; f) F. J. M. van de Ven, C. W. Hilbers, *Eur. J. Biochem.* **1988**, *178*, 1–38; g) S. S. Wijimenga, B. N. M. van Buuren, *Prog. Nucl. Magn. Reson. Spectrosc.* **1998**, *32*, 287–387.

[91] P. S. Asirvatham, V. Subramanian, R. Balakrishnan, T. Ramasami, *Macromolecules* **2003**, *36*, 921–927.

[92] A. C. J. de Dios, E. Oldfield, *J. Am. Chem. Soc.* **1994**, *116*, 5307–5314.

[93] E. Oldfield, *J. Biomol. NMR* **1995**, *5*, 217–225.

[94] C. W. Swalina, R. J. Zauhar, M. J. De Grazia, G. Moyna, *J. Biomol. NMR* **2001**, *21*, 49–61.

[95] G. Bifulco, L. Gomez-Paloma, R. Riccio, C. Gaeta, F. Troisi, P. Neri, *Org. Lett.* **2005**, *7*, 5757–5760.

[96] a) www.pdb.org; b) H. M. Berman, J. Westbrook, Z. Feng, G. Gilliland, T. N. Bhat, H. Weissig, I. N. Shindyalov, P. E. Bourne, *Nucleic Acids Res.* **2000**, *28*, 235–242.

[97] P. S. Eis, J. A. Smith, J. M. Rydzewski, D. A. Case, D. L. Boger, W. J. Chazin, *J. Mol. Biol.* **1997**, *272*, 237–252.

[98] C. Bassarello, P. Cimino, L. Gomez-Paloma, R. Riccio, G. Bifulco, *Tetrahedron* **2003**, *59*, 9555–9562.